Chapter

Functional Mechanism of Proton Pump-Type Rhodopsins Found in Various Microorganisms as a Potential Effective Tool in Optogenetics

Jun Tamogami and Takashi Kikukawa

Abstract

Microbial rhodopsins, which are photoreceptive membrane proteins consisting of seven α-helical structural apoproteins (opsin) and a covalently attached retinal chromophore, are one of the most frequently used optogenetic tools. Since the first success of neuronal activation by channelrhodopsin, various microbial rhodopsins functioning as ion channels or pumps have been applied to optogenetics. The use of light-driven ion pumps to generate large negative membrane potentials allows the silencing of neural activity. Although anion-conductive channelrhodopsins have been recently discovered, light-driven outward H^+-pumping rhodopsins, which can generate a larger photoinduced current than a light-driven inward Cl^--pump halorhodopsin, must be more efficient tools for this purpose and have been often utilized for optogenetics. There are abundant proton pumps in the microbial world, providing numerous candidates for potential practical optogenetic instruments. In addition, their distinctive features (that is, being accompanied by photoinduced intracellular pH changes) could enable expansion of this technique to versatile applications. Thus, intensive investigation of the molecular mechanisms of various microbial H^+-pumps may be useful for the exploration of more potent tools and the creation of effectively designed mutants. In this chapter, we focus on the functional mechanism of microbial H^+-pumping rhodopsins. Further, we describe the future prospects of these rhodopsins for optogenetic applications.

Keywords: Microbial rhodopsin, Photocycle, Proton transfer, Neural silencing, Optical pH control

1. Introduction

Optical control of biological reactions is one of the most recently studied fields of research because light facilitates highly spatial and temporal manipulation. In particular, optogenetics, that is, the specific and noninvasive control of biological activities such as neural activities by light stimulus of photoreceptor proteins heterogeneously expressed in targeted neurons or other related cells, has a significant impact in the field of neuroscience [1–8] and has attracted the interest of myriad

researchers in the life sciences. Over the past 15 years since the first report on optogenetics in 2005 [1], the development of tools for this interesting technique has been rapidly progressing [9–14]. Recently, various types of photosensitive proteins have been employed for optogenetics [15–17]. Nevertheless, retinal-based proteins found in microbes (referred to as microbial rhodopsins), which were first applied to optogenetics, are still overriding toolkits [18, 19].

Microbial rhodopsins (also termed type-I rhodopsins) are seven transmembrane α-helical proteins that bind to the retinal chromophore, similar to animal rhodopsins (also termed type-II rhodopsins) [20]. A distinctive property of animal rhodopsins is the difference in their chromophore configurations; retinals in microbial and animal rhodopsins adopt all-*trans* and 11-*cis* forms in the dark state, respectively. In addition, by all-*trans*-to-13-*cis* isomerization of the retinal with illumination, microbial rhodopsins undergo a linear cyclic photoreaction called photocycle, in contrast to animal rhodopsins, whose retinals are isolated from the protein moiety during their photoreaction processes. Their functions are also different; in addition to photo-sensing functions of animal rhodopsins, microbial rhodopsins also act as light dependent-ion transporters that can carry various types of ions such as H^+, Na^+, and Cl^- [21–24].

Microbial rhodopsins are classified into two categories of ion carriers. One is a light-gated ion channel, and the other is a light-driven ion pump. The former group includes channelrhodopsins (ChRs) [8, 25–27] and anion channelrhodopsins (ACRs) [28–30], which are the principal tools for optogenetics. Upon illumination, ChRs become permeable to various monovalent or divalent cations, such as H^+, K^+, Na^+, and Ca^{2+} [8, 25–27]. Therefore, in nerve cells expressing ChRs, the influx of Na^+ induced by light activation of ChRs causes depolarization in these cells, leading to neural activation [1–8, 25–27]. Conversely, light activation of ACRs, which act as anion-selective channels, can drive the hyperpolarization of ACR-expressing cells to suppress neural activity [28, 31]. The ion pump group includes light-driven outward H^+- [32, 33], Na^+- [34], and inward Cl^--pumps [35–38]. As these proteins can generate negative membrane potential in their incorporated cells by illumination, they can be utilized as neural silencers similar to ACRs [39, 40]. Microbial rhodopsins, as ion channels or pumps, can lead to changes in membrane potential by absorption of a photon without going through complicated reactions. This simple light-activated machinery makes them more easily applicable to optogenetics, together with repeatable properties through their photocycle.

Among the three types of ion-pumping rhodopsins, proton-pumping rhodopsins have a distinct feature from the other two. Proton translocation across the cell membrane induced by light activation of these pigments is accompanied by a change in intracellular pH. Hence, these proteins have the potential for various applications, for example, photoinduced pH control in cells or all sorts of organelles, as well as their use as neural silencers. To date, genes encoding H^+-pumping rhodopsins have been identified from the genomes of many microorganisms, irrespective of species [41], which enables us to gain the most plentiful genetic information from the database of the microbial rhodopsin family. Therefore, these types of rhodopsins may be applicable for exploring better candidates for optogenetics in various respects, such as the strength of neural inhibition, spectral properties (maximum absorption wavelength for activation), and kinetics.

Chow et al. screened efficient neuronal silencing rhodopsins and showed that the magnitude of photocurrents evoked by the activation of H^+-pump-type rhodopsins was on average higher than those evoked by the activation of inward Cl^--pump halorhodopsins (HRs) [39]. Moreover, the rates of activation upon light irradiation and recovery from inactivation after light cessation tended to be faster, as observed for archaerhodopsin-3 from *Halorubrum sodomense* (aR-3 or Arch), which is

currently the most powerful H^+-pumping tool for neural suppression, unlike HRs that retain long-lasting inactive states [39]. Based on these observations, H^+-pump rhodopsins are considered more effective for the light-induced inhibition of neurons. Thus, these experimental facts for the practical use of H^+-pumping rhodopsins have been steadily amassed; however, the utility of H^+-pumping rhodopsins for optogenetics has not been completely evaluated from the molecular viewpoint. Therefore, an overview of the molecular mechanism of various H^+-pumping rhodopsins, including newly found H^+-pumps, may be useful for further development and rational design of optogenetic instruments. Here, we describe the functional mechanism of H^+-pumping rhodopsins, particularly highlighting the aspect of photochemistry and the accompanying proton movement, with their future prospects for optogenetic applications.

2. H^+-pumping rhodopsins from various microbial species

2.1 H^+-pumps in archaebacteria

Among all microbial rhodopsins, the first H^+-pumping rhodopsin reported was bacteriorhodopsin (BR), which was discovered in *Halobacterium salinarum* living in salt lakes or salterns in 1971 [42]. Haloarchaea, including those described above, can survive even in extremely salty environments with low oxygen concentrations using BR-based phototrophy, which is accomplished by ATP synthesis driven through a proton gradient produced with outward proton translocation across the cell membrane. Haloarchaeal plasma membranes contain deeply purplish patches (referred to as purple membranes), in which BR forms highly dense assemblies in the form of a two-dimensional hexagonal lattice. The high BR expression in native membranes, along with its highly stable property, facilitated biochemical and biophysical investigations of this protein by various approaches, including spectroscopic and structural methods [32, 33, 43–48]. Thus, BR is the most well-studied H^+-pump.

Following the discovery of BR, the second H^+-pump identified was archaerhodopsin (aR). Two homologous proteins, archaerhodopsin-1 and -2 (aR-1 and aR-2), were simultaneously identified from *Halobacterium* sp. aus-1 and aus-2 isolated from a lake in Western Australia by Mukohata et al. [49]. Several aR homologous proteins, including aR-3 described above, have been discovered in different haloarchaeal species [50–53]. In addition, Mukohata et al. successively identified two other H^+-pump-like proteins belonging to a different clade from BR and aR: cruxrhodopsin-1 (cR-1) from *Haloarcula argentinensis* [54] and deltarhodopsin-1 (dR-1) from *Haloterrigena* sp. arg-4 [50]. Several homologs of these H^+-pumps have also been identified in other species [55–57]. aRs, cRs, and dRs are very similar H^+-pumps to BR; however, they are classified as apparently different tribes [50].

2.2 Eubacterial H^+-pumps

The history of microbial rhodopsin research has been confined to the archaebacterial world for about three decades since the first discovery of BR. However, since the 2000s, rapid technical advances in metagenomics have led to the discovery of unknown microbial H^+-pumping rhodopsins from various eubacteria [58, 59]. A representative example is proteorhodopsin (PR) from marine bacteria [60, 61].

In 2000, PR was first identified in the genome of uncultivated marine γ-proteobacteria, which is a member of the SAR86 clade, from a sea sample collected from Monterey Bay in California [62]. Thus, the nomenclature of this protein, i.e., "proteo-," originates from the name of the hosting bacterium. Sequencing of a bacterial artificial chromosome vector into which a fragmented DNA extracted from samples was cloned revealed the presence of a gene encoding rhodopsin-like protein (EBAC31A08) [62]. Furthermore, after transformation by this gene and successive induction of protein expression with exogenous retinal in *Escherichia coli*, acidification in suspension containing these PR-expressing cells was caused by illumination, indicating that PR can work as an outward light-driven BR-like H^+-pump in the *E. coli* membrane [62]. After the first discovery of PR, further surveys demonstrated the existence of genes encoding novel PRs in not only γ-proteobacteria but also α-proteobacteria containing ubiquitous marine clades such as the SAR11 group [63], β-proteobacteria [64], and Flavobacteria [65, 66]. In addition, genes encoding numerous PR variants (>several hundreds or thousands of variants) have been identified in widespread oceans [67–72]. Nowadays, most marine bacterioplankton living in the photic zone are assumed to hold PR genes [41]. PR can be classified into two groups depending on their absorption maxima (λ_{max}): green-absorbing PR (GPR), whose λ_{max} is approximately 525 nm, and blue-absorbing PR (BPR) with a λ_{max} of ca. 490 nm [67, 69, 73–75]. The difference between these two groups is probably associated with the adaptation to the environments that the PR-retaining bacteria inhabit; most bacteria that are distributed at the surface of the sea and have access to available green light have GPR to obtain energy produced effectively using this wavelength of light, while bacteria at the depth of the sea water that exclusively have access to available blue light contain BPR [67, 74, 75].

PR-related proteins were also discovered from non-marine bacteria present in various environments, such as freshwater [76], high mountains [77], hot springs [78], and permafrost [79]. For example, a PR-like protein identified from actinobacteria living in freshwater is called actinorhodopsin (ActR) because it is classified into a phylogenetically different clade from PR [76]. A halophilic eubacterium *Salinibacter ruber* also contains a PR-like H^+-pumping protein called xanthorhodopsin (XR) [80]. XR binds to the second chromophore, carotenoid salinixanthin, which acts as a light-harvesting antenna, expanding the spectral range for light activation of this protein because the energy obtained by light absorption of salinixanthin can be transferred to the retinal to induce isomerization [80, 81]. Another PR-like H^+-pump with binding ability to salinixanthin, similar to XR [82], was discovered from the cyanobacterium *Gloeobacter violaceus* and called *Gloeobacter* rhodopsin (GR) [83]. Furthermore, a new type of H^+-pump with a unique feature (described later) was discovered from a nonmarine gram-positive bacterium *Exiguobacterium sibiricum* present in Siberian permafrost samples, which was named *Exiguobacterium sibiricum* rhodopsin (ESR) [79]. Thus, PR-like eubacterial H^+-pumping rhodopsins have been found in various archaea and bacteria [84, 85] and even in eukaryotic marine protists [86], which seems to have been achieved by lateral gene transfer [84].

2.3 Two types of H^+-pumps from lower eukaryotes

In 1999, the presence of a gene encoding eukaryotic microbial rhodopsin (*nop-1*) was first found in the eukaryotic filamentous fungus *Neurospora crassa* [87]. This rhodopsin-like protein encoded by *nop-1* is called *Neurospora* rhodopsin (NR). The amino acid sequence of NR contained the requisite corresponding residues for proton pumping of BR; however, a previous photochemistry study using

recombinant NR proteins heterogeneously expressed in the methylotrophic yeast *Pichia pastoris* revealed that NR showed a slower photocycle that is close to sensor-type rhodopsins [88]. Therefore, it is speculated that NR is physiologically associated with carotenoid biosynthesis regulation by functioning as a photosensor rather than a H^+-pump [89, 90], although its exact physiological role remains unknown. Later, other NR-related fungal opsin genes were discovered in a different fungal species, *Leptosphaeria maculans*, which is the fungal agent of blackleg in canola [91]. This opsin-coded protein is termed *Leptosphaeria* rhodopsin (LR or Mac). Through its characterization using proteins prepared by heterogeneous expression in yeast (*Pichia pastoris*) similar to NR, it was demonstrated that LR acts as a BR-like outward H^+-pump with a fast photocycle, unlike NR [91]. Furthermore, through advanced genomic analyses, new fungal rhodopsins that are classified into a third subgroup were identified. The fungal wheat pathogen *Phaeosphaeria nodorum* possesses two rhodopsin-like protein-encoding genes [92]. These fungal rhodopsins are called *Phaeosphaeria* rhodopsin 1 (PhaeoRD1) and *Phaeosphaeria* rhodopsin 2 (PhaeoRD2). PhaeoRD1 is an analogous protein to LR, whereas PhaeoRD2 is a member of the third group. Considering its coexistence with other rhodopsin forms from the same species, PhaeoRD2 is regarded as an auxiliary protein [92]. Characterization of these fungal rhodopsins heterogeneously expressed in *P. pastoris* suggested that both pigments exhibit fast photocycles that are characteristic of H^+-pump-type rhodopsins [92].

Acetabularia rhodopsin (AR) is another eukaryotic H^+-pump found in the giant unicellular marine green alga *Acetabularia acetabulum* [93]. *Acetabularia acetabulum*, which is also known as the "Mermaid's Wineglass", is an extremely interesting organism in terms of morphology because this unicell exhibits a unique complex life cycle comprising several distinct developmental phases [94]. In 2004, Mandoli et al. first reported the cDNA sequence of a fragmented possible opsin-encoding gene

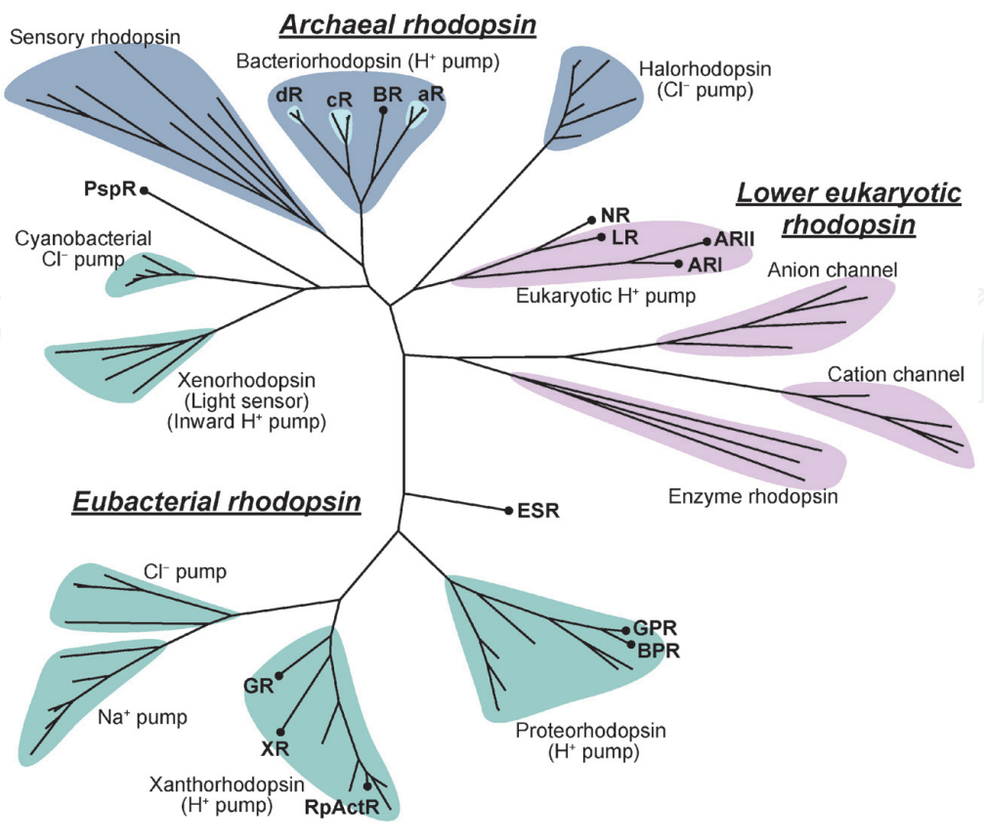

Figure 1.
Phylogenetic tree of microbial rhodopsins. RpActR represents ActR from actinobacterium Rhodoluna planktonica strain MWH-Dar1.

(*aop*) from juvenile *Acetabularia*. Subsequently, Hegemann et al. succeeded in cloning full-length opsin cDNA from this alga [93]. They heterogeneously expressed AR proteins in the membrane of *Xenopus laevis* oocytes and characterized the electrophysiological properties of this protein. Through a series of experiments, they demonstrated that AR is an outward light-driven H^+ pump [93]. Moreover, Jung et al. successively recloned two opsin genes from juvenile *Acetabularia*, which slightly differed from the gene cloned by Hegemann et al. The two AR homologs identified by them were named *Acetabularia* rhodopsin I and II (ARI and ARII, also abbreviated as Ace1 and Ace2, respectively) [95, 96]. Thus, two types of H^+-pumps from eukaryotic microorganisms are currently known: fungal and algal H^+-pumping rhodopsins (**Figure 1**).

3. Proton translocation mechanism of microbial H^+-pumping rhodopsins: from the photochemical and proton transfer viewpoints

3.1 Proton transport of BR: a typical model of H^+-pumping rhodopsins

When the molecular mechanism of microbial H^+-pumping rhodopsins is considered, the scenario of proton transportation in BR is often used as a prototype. Detailed descriptions of the H^+-pumping mechanism of BR from various aspects can be found in excellent previously published reviews (refer to relevant refs. [32, 33, 43-48]). We present only a brief outline here.

The photocycle of BR is initiated by photoisomerization of the retinal from all-*trans* to 13-*cis* upon formation of the K-intermediate. Then, during the transition between four sequentially formed photoproducts, L, M, N, and O intermediates, stepwise proton transfer reactions occur between amino acid residues buried within the protein or aqueous phases on both the cytoplasmic (CP) and extracellular (EC) sides. In these processes, three main groups play an essential role in proton transport. One is a part of the retinal Schiff base (SB), which represents a linkage with a specific lysine residue located at the center of the seventh helix of the protein (G-helix) ($Lys216^{BR}$, **Figure 2**). This portion is usually protonated in the unphotolyzed state (protonated retinal Schiff base, PSB). The other groups are two aspartic acid residues, $Asp85^{BR}$ and $Asp96^{BR}$, located in the EC and CP domains, respectively, on the C-helix. $Asp85^{BR}$ facilitates the first step of proton translocation upon the L–M transition as a proton acceptor from PSB, whereas $Asp96^{BR}$ works as a proton donor to deprotonated SB during M–N transition and is sequentially involved in proton uptake from the CP bulk upon N–O transition accompanied by 13-*cis*-to-all-*trans* retinal reisomerization. Both $Asp85^{BR}$ and $Asp96^{BR}$ are required for efficient proton pumps because substitutions of these residues with nonionizable residues abolished or significantly decreased H^+-pumping capability [97].

A proton releasing complex (PRC) comprising several internal H_2O and various residues on the EC surface such as $Tyr57^{BR}$, $Arg82^{BR}$, $Tyr83^{BR}$, $Ser193^{BR}$, $Glu194^{BR}$, $Glu204^{BR}$, and $Thr205^{BR}$ also participates in the proton transfer reaction of BR [98, 99], although it is not always an indispensable component for proton pumping. The pK_a value of PRC in the H^+-releasing M-state ($\sim$6) [100] divides the timing of proton release into two patterns: at pH values above $\sim$6, a proton is initially released from PRC to the EC bulk during the L–M transition and the resultant deprotonated PRC receives a proton from the protonated $Asp85^{BR}$ upon O-decay. In contrast, at pH values below $\sim$6, the first such proton release from PRC upon M-rise does not occur, and a proton on PRC is released late upon O-decay [101].

Two threonine residues, $Thr89^{BR}$ and $Thr46^{BR}$, are also important, although these residues do not belong to the series of proton transfer events due to

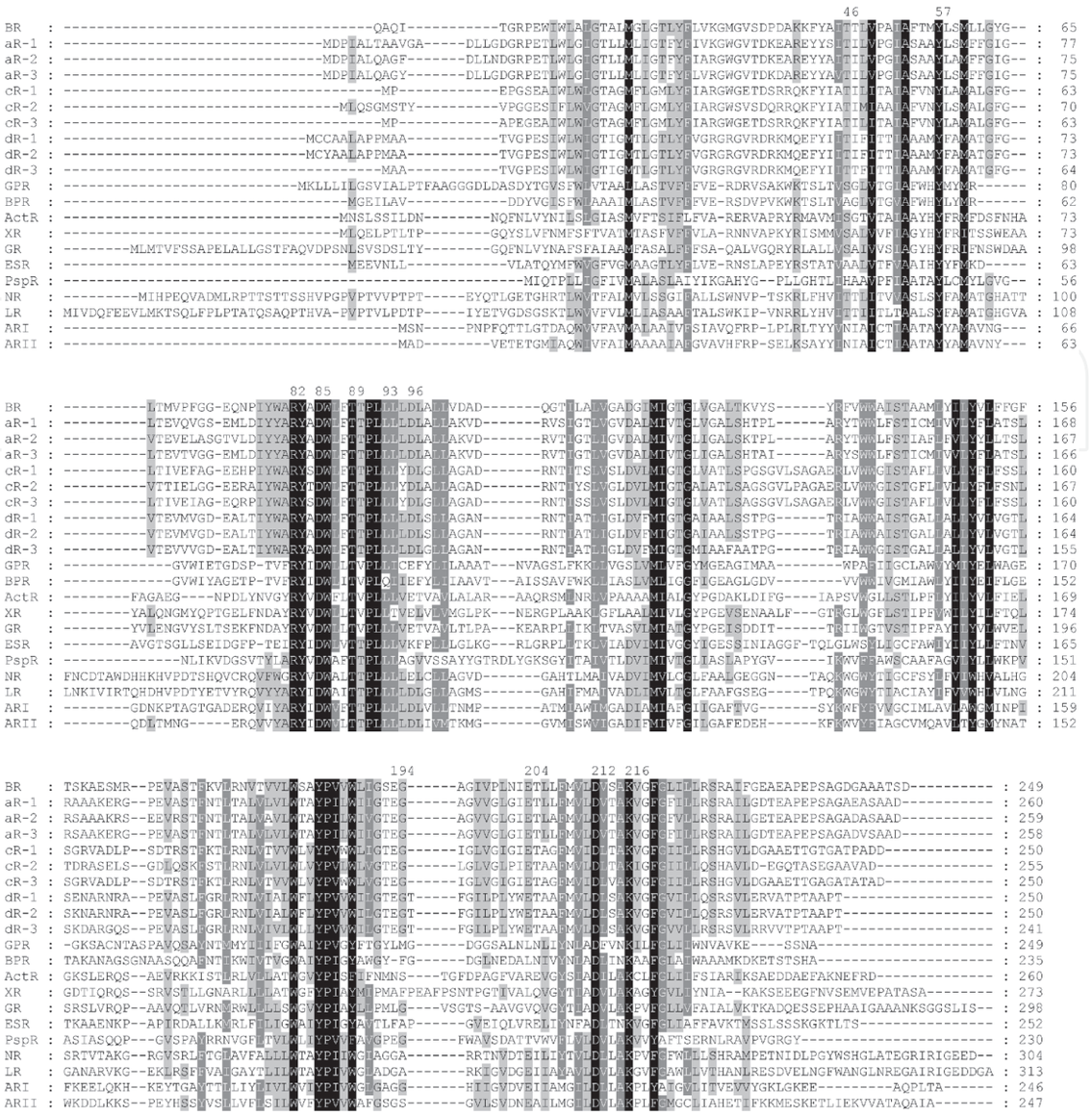

Figure 2.
Amino-acid alignment of various microbial H⁺-pumping rhodopsins. Analysis was performed using a multiple sequence alignment program (CLUSTALW). The numbers shown in the top row represent the numbering of amino acid residues in BR. The dotted line represents the missing residues in the determined structure. The amino acid residues with maximum homological numbers at each position are marked with a black or gray background depending on their numbers: The monochrome tone becomes darker as the number of homological residues increases. Notes: cR-2, cR from Haloarcula sp. arg-2; cR-3, cR from Haloarcula vallismortis; dR-2, dR from Haloterrigena turkmenica JCM9743; dR-3, dR from Haloterrigena thermotolerans; GPR, γ-proteobacterium (EBAC31A08) GPR; BPR, γ-proteobacterium (Hot75m4) BPR; ActR, RpActR.

nonionizable residues. Thr89^{BR} is within the active center and includes PSB, Asp85^{BR}, and some water molecules [102], where this residue forms a hydrogen bond with Asp85^{BR} [103], indirectly contributing to the initial proton transfer from PSB to Asp85^{BR} during M-formation [102, 103]. In contrast, Thr46^{BR} forms an interhelical hydrogen bond with Asp96^{BR} in the CP region, which is associated with the regulation of pK_a in Asp96^{BR} in the unphotolyzed state [104].

3.2 Common and different points on the amino-acid sequences among varying H⁺-pumps

In most outward H⁺-pumping microbial rhodopsins identified to date, the residues corresponding to three main groups (PSB [Lys216^{BR} as the retinal binding site], Asp85^{BR}, and Asp96^{BR}) described above are highly conserved. By checking their

presence, we can therefore forecast whether each protein in the microbial rhodopsin family acts as an H^+-pump like BR. **Figure 2** shows a comparison between important amino acid residues for proton transport among representative H^+-pumping rhodopsins. As shown in this figure, almost all primal residues relevant to proton transport in archaeal-type H^+-pumps agree with the residues corresponding to BR. Similarly, both fungal and algal H^+-pumps from eukaryotes retain the residues corresponding to $Asp85^{BR}$ and $Asp96^{BR}$; however, a difference exists in the components of PRC in BR. In both types of eukaryotic H^+-pumps, the residue corresponding to $Glu194^{BR}$ of two EC glutamates in PRC is replaced by glycine, whereas another residue corresponding to $Glu204^{BR}$ is conserved. In contrast, in the eubacterial H^+-pump, the residues corresponding to $Asp96^{BR}$ are substituted by conservative carboxylate glutamic acid, although there are several exceptions. Another significant aspartate corresponding to $Asp85^{BR}$ is perfectly conserved, similar to other types of H^+-pumps. Furthermore, these H^+-pumps lack both glutamic acids in the components of PRC: $Glu194^{BR}$ and $Glu204^{BR}$. Thus, a comparison of the amino acid sequences among various H^+-pumping rhodopsins can reveal the superconservation of the proton acceptor ($Asp85^{BR}$) and the diversity of the proton donor ($Asp96^{BR}$) and the residues in the EC proton releasing pathway. These differences could lead to different methods of proton transfer among varying H^+-pumps.

3.3 Photocycles of other H^+-pumping rhodopsins than BR

During a single photocycle induced by the absorption of one photon, ion-pump-type rhodopsins can transport ions as substrates. The number of photocycle turnover under illumination, therefore, affects the amount of ions transported by these proteins, in other words, the ion-pumping activity of these rhodopsins. In general, the turnover rate of the photocycle in ion-pumping rhodopsins tends to be relatively higher than those of photosensor-type rhodopsins to transport numerous ions per illumination. The speed of their photocycle completion can be used to analyze the H^+-pump, in addition to actually measuring H^+-pumping activity that is usually examined by measuring the photoinduced pH change in a suspension of cells expressing these rhodopsins. Furthermore, the identification of photointermediates during the photocycle of respective rhodopsins and the estimation of their rise/decay kinetics together with the measurement of transient proton transfer during their photocycles enable us to understand the timing of proton movement. Thus, detailed investigations of the photocycles are important for understanding the H^+-pumping mechanism.

Among the H^+-pumping rhodopsins identified so far, the next well-characterized proton pump following BR is GPR. In many studies, the first identified PR variant (EBAC31A08) was employed as a sample. As soon as GPR was discovered in 2000, various spectroscopic approaches such as static and time-resolved transient UV–visible, FTIR, and FT-Raman spectroscopies were applied to characterize the photochemistry of this protein, as previously performed for the research of BR [105–110]. These experimental results revealed that the photocycle of GPR was similar to that of BR but also concomitantly contained several differences. Using the same kinetically analytical method as previously applied to the transient absorbance data of BR, where the possibilities of parallel or branch models were also considered [111], Váró et al. determined the photocycles of GPR at acidic and alkaline pH values [108, 109]. Their proposed photocycle at alkaline pH (9.5) is in accordance with the following scheme: $GPR \rightarrow K \leftrightarrow M_1 \rightarrow M_2 \leftrightarrow N \leftrightarrow GPR'(O) \rightarrow GPR$ [108]. As shown in the above scheme, one of the apparent differences from the BR photocycle is the absence of L after K, which is thought to be probably due to kinetic reasons. A remarkably retarded (ca. 10-100-fold slower) decay of K compared with that of BR was observed in GPR [105]. Because of such slow K-decay,

low-temperature Raman spectroscopic data presented by Fujisawa et al. demonstrated that the chromophore structure in GPR in the K state is less distorted compared to that of BR in the same state and is rather close to that of L in BR, which possess a more relaxed chromophore structure [112]. Therefore, the formation of a longer stable K state may obscure the appearance of L in the GPR along with the fast formation of the following M-state. Another difference from BR can be observed in the spectral characteristics of the latter photoproducts, N and GPR'(O). The N-intermediate in PR was red-shifted with 13-*cis* chromophore retinal [105, 108] and resembled O in BR with respect to the absorption maxima. In addition, the GPR' intermediate had all-*trans* retinal chromophores similar to O in BR; however, its λ_{max} was very close to that of the original pigment. Friedrich et al. also determined the photocycle of GPR under both acidic (pH 5) and alkaline (pH 10) conditions based on a global fitting analysis (sequential irreversible model) for flash photolysis data [106]. In the latter half of the photocycle scheme proposed by them, after an equilibrium of M and a red-shifted O (λ_{max} = 580 nm) was produced, an equilibrium of N with a spectral property similar to that of the original pigment (λ_{max} = 530 nm) and O appeared [106]. Hence, if it is assumed that O and N in their scheme agree with N and GPR' in Váró's scheme, respectively, both schemes are compatible. The rate of photocycle turnover in GPR was fast (<several hundreds of milliseconds), although it was somewhat slower than that of BR (<several tens of milliseconds). In contrast, the photocycle of another type of PR, BPR, was slower by an order of magnitude than that of GPR [113]. The possibility of using BPR as a photosensor has been advocated, although its physiological role is still debated [113].

The photocycles of other eubacterial H^+-pumping rhodopsins, including XR, GR, ESR, and ActR, were also investigated by time-resolved absorption spectroscopy [80, 83, 114–116]. Their photocycles go through the K, L, M, N, and O states, similar to BR or GPR. For many eubacterial H^+-pumps including GPR, structural information obtained by multiple approaches such as X-ray crystallography, NMR, and atomic force microscopy has also been reported [117–123], providing structural insights into their photochemistry.

Recent genome analysis revealed that numerous eukaryotic fungi possess rhodopsin-like protein-encoding genes (RDs) and opsin-related genes (ORPs) [124]. Nevertheless, unlike archaeal or bacterial H^+-pumping rhodopsins, reports on the photochemistry of eukaryotic H^+-pumps are extremely limited because the protein expression in *Pichia pastoris* has been established only for a few fungal rhodopsins such as NR and LR. Meanwhile, several studies on the photochemical characterization of LR and its analogous protein PhaeoRD1 using visible and infrared spectroscopic techniques have been published [91, 92, 125–128]. These reports revealed that their photocycles include the K, L, M, N, and O states, similar to the BR photocycle [91, 92].

For two algal H^+-pumps, ARI and ARII, the establishment of a large-scale sample preparation method using a unique *Escherichia coli* cell-free membrane-protein production system developed by Shimono et al. [129] allowed the detailed elucidation of the spectroscopic and structural features of these proteins [96, 130–133]. Through global fitting analysis for time-dependent absorption changes based on a sequential irreversible model, we determined that the photocycles for ARI and ARII at near-neutral pH values can be represented by ARI → K↔L↔M↔N↔O → ARI' → ARI and ARII→K → L↔M↔N↔O → ARII' → ARII, respectively, which are very similar to the BR photocycle [130, 131]. However, the formation of a long M-N-O quasi-equilibrium was observed in both the photocycles of both AR proteins [130, 131], which is characteristic of these ARs. This indicates the presence of pronounced reverse reactions between M, N, and O in the photocycles of ARI and ARII. Although similar N–M or O–N back reactions also exist in BR, the rates of these reactions in BR are not significantly higher than those of ARI and ARII. The

existence of prompt back reactions could hamper the fast turnover of the photocycle in these rhodopsins, thereby reducing H^+-pumping efficiency. However, a significantly faster O-rise and the irreversibility of the transitions from O to ARII' (a precursor of ARII) and from ARII' to the original state were observed during the photocycle of ARII [130]. Owing to these kinetic properties, the overall photocycle of ARII is a forward reaction, which may result in a turnover rate ($<\sim$100 ms at neutral pH) that is comparable to that of BR [130]. In contrast, the photocycle turnover of ARI was approximately 10-fold slower than that of ARII [131]. This may be attributed to slower decay of O and ARI' in the second half of the photocycle in ARI compared to the decay of O and ARII' in the photocycle of ARII.

3.4 Initial proton transfer from PSB to the proton acceptor, aspartate, upon L–M transition: the most crucial step for proton transport

As described above, the proton acceptor residue from PSB corresponding to $Asp85^{BR}$ is superconserved in all H^+-pump-type rhodopsins, suggesting the significance of this residue in the proton pumping mechanism. The negative charge of deprotonated $Asp85^{BR}$ interacts with another deprotonated aspartate $Asp212^{BR}$ and three water molecules through hydrogen bonds, forming a pentagonal cluster that electrostatically stabilizes two positive charges of PSB and $Arg82^{BR}$ [47]. The same cluster structure has also been observed in H^+-pumping rhodopsins other than BR [22, 131]. In this sense, two aspartates also play an important role in counterions to PSB, in which $Asp85^{BR}$ and $Asp212^{BR}$ are referred to as primary and secondary counterions, respectively. The aspartate residue, which is the proton acceptor, is deprotonated in the unphotolyzed state under physiological conditions. At pH values below the pK_a of the proton acceptor in the resting state, where this residue takes the protonated form, initial proton migration from PSB does not occur; thus, the formation of the M state with deprotonated SB is not observed and H^+-pumping activity vanishes. The pK_a of the proton acceptor in the unphotolyzed state, therefore, tends to adopt as low a value as possible, for example, ca. 2.5 for $Asp85^{BR}$ [134]. $Asp85^{BR}$ is conjugated with PRC located on the EC surface, which contributes to the retention of its low pK_a in the dark state [45, 134].

In contrast, the pK_a values of proton acceptor residues in eubacterial H^+-pumps tend to be relatively higher, for example, approx. 7-7.5 for GPR [105, 106, 109, 113], 7.8 (or 6.2) for BPR [113], 6.0 for XR [135], 4.5 for GR [136], 6.0 for ESR [137], and 5.8 for ActR [116]. Such high pK_a values in these pigments are thought to be associated with physiological pH conditions of the hosting bacteria possessing these rhodopsins; because the habitat of bacteria containing PR-like proteins (e.g., sea water, freshwater, etc.) usually has near-neutral or weakly alkaline pH conditions (approx. pH 6.5-8.5) that are above the pK_a values of the proton acceptors in the dark state, the proton acceptors of these H^+-pumps can adopt the deprotonated form to work as proton pumps. The elevated pK_a values of the proton acceptors in eubacterial-type H^+-pumps may be due to the absence of two EC glutamates corresponding to $Glu194^{BR}$ and $Glu204^{BR}$ and the repositioning of an arginine residue (corresponding to $Arg82^{BR}$) located within the pentagonal cluster in the EC channel [138]. Moreover, in GPR, it was clarified that a highly conserved histidine residue $His75^{GPR}$ among bacterial H^+-pumps that is adjacent to the proton acceptor $Asp97^{GPR}$ contributes to the adjustment of the higher pK_a of $Asp97^{GPR}$ in the unphotolyzed state because the mutation of this residue significantly decreases the pK_a of $Asp97^{GPR}$ [139]. The replacement of the corresponding histidine residues in other eubacterial H^+-pumps, however, did not cause such a large change in the pK_a of their proton acceptor residues [136, 137], implying that the above-mentioned pK_a modulation mechanism through histidine is not common in all eubacterial-type H^+-pumps.

The primary and secondary counterions (corresponding to $Asp85^{BR}$ and $Asp212^{BR}$, respectively) are located near and arranged symmetrically around the PSB, resulting in forming a part of the proton acceptor cluster. The secondary counterion is also deprotonated like the primary counterion (proton acceptor) because the pK_a of this residue in the resting state usually takes a further lower value compared to the primary counterion. Nevertheless, a proton of PSB is always transferred to the primary counterion at the photoproduct rather than the secondary counterion. How should this proton transfer mechanism be considered? In the case of BR, it is thought that upon L–M transition, the pK_a of PSB is lowered from a value above ~13 in the dark state to a value below ~3, which is near the pK_a (~2.5 [134]) of $Asp85^{BR}$ in the same state. In contrast, the pK_a of $Asp85^{BR}$ simultaneously increases to a value of at least 8.5 approximately at this time (the first increase in the pK_a of $Asp85^{BR}$) [140]. Thus, the pK_a values between PSB and $Asp85^{BR}$ are reversed, giving rise to a one-way proton movement from PSB to the deprotonated $Asp85^{BR}$. Then, the pK_a of $Asp85^{BR}$ finally increases to above ~10 in the M-state, thus allowing it to maintain its protonated state until the end of the photocycle (a second increase in the pK_a of $Asp85^{BR}$) [140]. The second increase in the pK_a of $Asp85^{BR}$ upon M-formation is thought to be triggered by the disruption of the electrostatic interaction between the negatively charged $Asp85^{BR}$ and the positively charged $Arg82^{BR}$ in PRC, which is caused by the protonation of $Asp85^{BR}$ and the accompanying deprotonation of PRC (initial proton release from PRC) during this process [140].

In contrast, a question that could arise would be how pK_a regulation in the proton acceptors of PR-like eubacterial H^+-pumps lacking their coupled PRC is achieved. Although there is no experimental evidence, we may presume that a similar pK_a inversion between PSB and its proton acceptor ($Asp97^{GPR}$) in BR occurs upon the formation of M in GPR; the pK_a of PSB decreases from $> \sim 11$ in the unphotolyzed state [141] to ~3 upon M-rise, resulting in it being lower than the pK_a of $Asp97^{GPR}$ in the dark state (7-7.5). The possibility of an increase in the pK_a of $Asp97^{GPR}$ in the M-state similar to BR has also been reported [142]. FTIR data in DMPC-reconstituted vesicles revealed that the origin of the first proton release upon M-rise observed in GPR under alkaline conditions (pH ~9.5) is not $Asp97^{GPR}$, which is protonated during this transition [142]. This observation implies that the pK_a of $Asp97^{GPR}$ at M is above ~9.5. Why is the photoinduced pK_a increase in $Asp97^{GPR}$ caused by the absence of a BR-like interaction with PRC? Although the reason is still unclear, an alternative interaction with neighboring $His75^{GPR}$ [143] may work instead of the PRC, which is missing in GPR.

Through low-temperature FTIR experiments, it was suggested that PSB forms a stronger hydrogen bond with $Asp227^{GPR}$ rather than $Asp97^{GPR}$ within the pentagonal cluster around PSB upon K-formation [144]. In addition to this observation, the pK_a of $Asp227^{GPR}$ in the unphotolyzed state was estimated to be approximately 2.6 or 3.0 [141, 145]. Hence, we cannot exclude the possibility that $Asp227^{GPR}$ receives a proton from PSB at the photoproduct under such low pH conditions ($\sim 3 <$ pH $< \sim 7$), where $Asp97^{GPR}$ and $Asp227^{GPR}$ are protonated and deprotonated at the resting state, respectively. Our experimental data using a rapid time-resolved pH-sensitive electrode method (described later with the details of this experimental method), however, showed that the pK_a of $Asp227^{GPR}$ may further decrease from ~3 at the dark state to ~2.3 at the photolyzed state [145]. This possible pK_a decrease in $Asp227^{GPR}$ at the photoproduct might hinder its proton acceptance from the PSB. Even though $Asp227^{GPR}$ can transiently receive a proton from PSB, the proton might be immediately released to other dissociable residue(s) or internal waters. Interestingly, the computational calculations performed by Bondar et al. suggested that among three possible pathways of proton transfer from PSB to $Asp85^{BR}$, that is,

1) a direct pathway to $Asp85^{BR}$ on the $Thr89^{BR}$ side of the retinal, 2) a proton wire through $Thr89^{BR}$, and 3) a proton transfer pathway via $Asp212^{BR}$, the energy barrier of the third proton transfer pathway was the smallest [146]. Thus, a similar photo-induced pK_a decrease in the second counterion to GPR occurs even in other H^+-pumping rhodopsins, including BR, and might play a role in the initial proton movement from PSB to its proton acceptor upon light activation of these pigments. Further studies are required to clarify the roles of this mechanism.

3.5 Diverse proton transfer occurring on the CP side

Following the EC proton transfer in the first half of the photocycle, the CP proton transfer events via the SB proton donor in the second half of the photocycle after M-decay are the next critical steps. The proton transfer mechanism at this stage varies among the three types of H^+-pumping rhodopsins—archaeal, bacterial, and eukaryotic. In the latter half of the BR photocycle, the deprotonated SB first accepts a proton from its proton donor, $Asp96^{BR}$, located in the CP channel during the M–N transition. The pK_a of SB in this reprotonation process was estimated to be approximately 8 [147]. In contrast, the pK_a of $Asp96^{BR}$ is maintained at a higher value ($> \sim 11$) through an interhelical hydrogen bond with $Thr46^{BR}$ on the B-helix [148]. Therefore, the pK_a of $Asp96^{BR}$ needs to be lower than the pK_a value ($\sim$8) of SB to release a proton toward deprotonated SB, from $> \sim 11$ at the initial state to $\sim$7-7.5 [149, 150]. This pK_a decrease is caused by the entry of water with the opening of the intracellular segment via the outward tilt of the F-helix at the M-state, leading to the internal hydration of the CP region. The inflow water breaks the interaction between $Asp96^{BR}$ and $Thr46^{BR}$, facilitating hydrogen bonding rearrangement so that $Asp96^{BR}$ forms a new interaction with neighboring water chains [151]. Then, during the following N–O transition, the pK_a value of $Asp96^{BR}$ increases again and finally reaches a higher value ($> \sim 11$) close to one in the dark state. Therefore, $Asp96^{BR}$ can capture a proton from the CP medium to reprotonate.

As described above, in GPR, the residue corresponding to $Asp96^{BR}$ is the conservative carboxylate, $Glu108^{GPR}$. This residue can function as a proton donor to SB; however, the proton movement from $Glu108^{GPR}$ to SB and the subsequent reprotonation of $Glu108^{GPR}$ from the CP bulk are indistinguishable, unlike BR; two sequential proton transfer events in the CP channel concurrently take place upon the M–N transition [105]. The difference in CP proton migration in eubacterial H^+-pumps, including PR from BR, seems to be related to the difference in the environment around the proton donor in the intracellular part of the protein between them. In many eubacterial H^+-pumping rhodopsins, the interhelical hydrogen bonding pair corresponding to the Asp-Thr interaction in BR is replaced by the Glu-Ser interaction. The X-ray crystal structure of XR in the dark state revealed that the proton donor ($Glu107^{XR}$) in the CP channel connects to the peptide carbonyl of the lysine residue ($Lys240^{XR}$) in SB; therefore, the CP H-bonded chain via water is already formed in the unphotolyzed state [118]. Thus, the difference in the CP proton transfer scheme from BR may be due to the formation of the hydrophilic CP pathway in eubacterial H^+-pumps.

We also observed a further interesting characteristic in the CP proton transfer of the PR-like H^+-pump ESR. The residue positioned at the site of the proton donor in ESR is the cationic residue $Lys96^{ESR}$ (see **Figure 2**). Nevertheless, $Lys96^{ESR}$ seems to be involved in the CP proton transfer from the intracellular aqueous space to the inner deprotonated SB because the replacement of this residue by other nonionizable residues resulted in a significant delay of the M-intermediate [114]. This observation exploded a conventional concept, the so-called carboxyl rule, that

the functional proton-donating residue is confined to two carboxylates (Asp or Glu). Some distinct structural features of BR can be observed in the X-ray crystal structure of the ESR. One of the differences is the presence of a cavity around $Lys96^{ESR}$ located close to the CP bulk media [122]. Although $Lys96^{ESR}$ is surrounded by hydrophobic residues in the CP channel in the dark state similar to BR, the cavity in the vicinity of $Lys96^{ESR}$ is separated only by a polar side chain of $Thr43^{ESR}$ (corresponding to $Phe42^{BR}$), in contrast to BR, whose proton donor residue is completely separated from the CP bulk solvent by a hydrophobic barrier composed of multiple hydrophobic residues including $Phe42^{BR}$ [122]. Connectivity with the CP bulk facilitates direct access of the protons from the CP solvent in $Lys96^{ESR}$. Another difference is the flexibility of the side chain of $Lys96^{ESR}$, which may allow the smooth repositioning of this residue by donating to SB and reprotonation. Given that these structural properties are present in the CP region together with the time-resolved spectroscopic data using D_2O, it may be plausible that the CP proton transfer scheme in ESR is as follows [114]: $Lys96^{ESR}$ adopts an unprotonated form at the resting state to be buried within the hydrophobic CP region. Upon M-decay, $Lys96^{ESR}$ transiently catches a proton from the CP bulk solvent (at $M_1 \leftrightarrow M_2$), and then, a little later, it donates a proton to SB (at $M_2 \leftrightarrow N_1$). Hence, $Lys96^{ESR}$ acts as a residue facilitating proton delivery from the CP bulk to the SB, which is an apparently different proton donating mechanism from the conventional one.

Another unique example of CP proton transfer was found in two types of gram-negative rod-shaped Proteobacteria in soil: *Pseudomonas putida* rhodopsin (PspR) from *Pseudomonas putida* and *Pantoea ananatis* rhodopsin (PaR) from *Pantoea ananatis*, a plant pathogen [152]. The notable properties of these types of rhodopsins are the replacement of the residue corresponding to $Asp96^{BR}$ with nonionizable glycine and the presence of a specific histidine at the position corresponding to $Thr46^{BR}$. This histidine residue is highly conserved in a member of this group and is assumed to constitute a part of a proton-donating complex [152]. However, it was observed that the rate of M-decay linearly depends on the proton concentration of the medium in a homologous protein in the same group [153], implying that the histidine forms a CP conductive channel rather than a proton-donating complex to enable rapid proton movement from the CP surface. Identification of the role of this unique histidine requires further study.

Among eukaryotic H^+-pumps, both fungal and algal H^+-pumps possess the same proton donor aspartate residue as BR. For two algal H^+-pump homologs ARI and ARII, however, the residue corresponding to $Thr46^{BR}$ is replaced by asparagine, which may cause different interactions with the proton donor and its pK_a regulation from BR and fungal-type rhodopsins. Our experimental data indeed revealed that the pK_a values of their proton donors ($Asp100^{ARI}$ and $Asp92^{ARII}$) in H^+-uptake (N-O transition) are ~6 (**Figure 3D**), which is ca. 1-1.5 units lower than that of BR (7-7.5) [130]. In the sensor-like fungal rhodopsin NR, the residue corresponding to $Asp96^{BR}$ is glutamic acid, similar to numerous eubacterial H^+-pumping rhodopsins, while the corresponding residue in the H^+-pump LR is aspartic acid, similar to BR. Interestingly, the substitution of the proton donor $Asp150^{LR}$ with an NR-like glutamate abolished the fast H^+-pumping photocycle [126, 127], implying that residues other than native aspartate work improperly in fungal H^+-pumps, even though it is a conservative one. In contrast, the influence of Asp-Glu replacement in $Asp96^{BR}$ differed depending on the experimental conditions [97, 154]. In the reconstituted BR heterogeneously expressed in *Escherichia coli*, the replaced glutamate residue fully functioned as a proton donor [97], whereas the replacement of BR in the native membrane led to a remarkable delay in SB reprotonation [154]. In contrast to the cases of BR or LR, the proton donating function of GPR was not lost by the

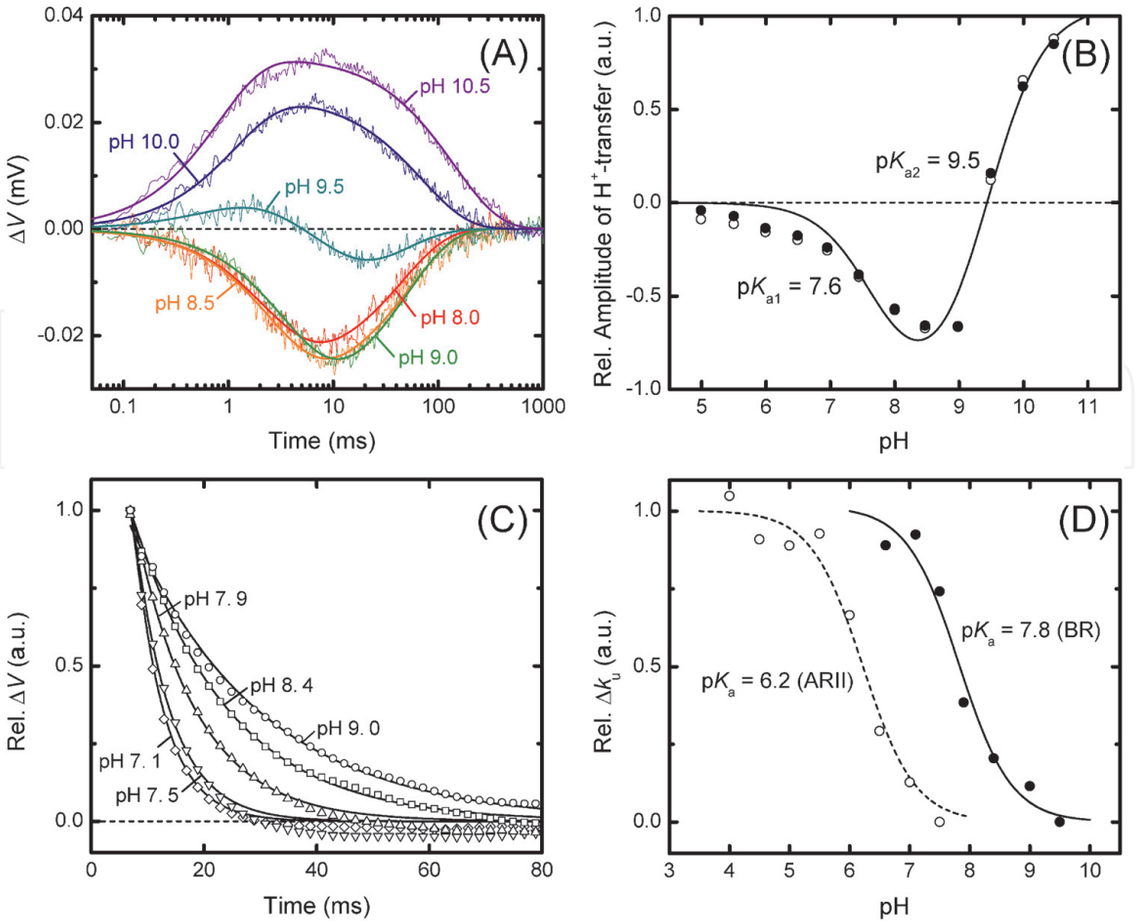

Figure 3.

pK_a estimation of critical residues for a proton pump by the SnO_2 (or ITO) electrode method. (A) Photoinduced voltage changes representing proton uptake/release at varying pH values [164]. Noisy and smooth curves represent the observed and fitted curves, respectively. For fitting, we employed the following kinetic equation: $\Delta Voltage \propto \Delta[H^+] = -A\frac{k_{f,u}}{k_{s,r}-k_{f,u}}\left(e^{-k_{f,u}t}-e^{-k_{s,r}t}\right)+B\frac{k_{f,r}}{k_{s,u}-k_{f,r}}\left(e^{-k_{f,r}t}-e^{-k_{s,u}t}\right)$*, where A represents a constant reflecting the fraction of the subpopulation photoinducing the first proton uptake followed by release and the rate constants of the first H^+-uptake and second H^+-release in such a proton transfer sequence are expressed by $k_{f,u}$ and $k_{s,r}$, whereas B represents a constant reflecting the fraction of subpopulation inducing the opposite sequence of proton transfer, and the rate constants of the first H^+-release and second H^+-uptake in that case are expressed by $k_{f,r}$, and $k_{s,u}$, respectively. At pH < 9.5, where the first H^+-release cannot be obviously observed, it was assumed that B is almost zero. In contrast, the fitting at pH > 9.5 was conducted as A = 0. Six buffer agents with different pK_a values were added to the media for experiments so that the buffering action remained constant over a wide pH range (~5 ≤ pH ≤ ~11). (B) Plot of amplitude of H^+-transfer versus pH. Filled and empty circles indicate plots of strict values with theoretical regression (−A and B values obtained by the above fitting) and approximate peak values of photoinduced signals estimated by sight, respectively. These values were plotted as relative values. A solid curve represents a curve fitted using the following equation:* $\Delta[H^+] = -C\left(\frac{1}{1+10^{pK_{a1}-pH}}\right)\left[\left(\frac{1}{1+10^{pH-pK_{a2}}}\right)-\left(\frac{1}{1+10^{pK_{a2}-pH}}\right)\right]$*, where C, pK_{a1}, and pK_{a2} represent a scaling constant for the amplitude, pK_a values of $Asp97^{GPR}$, and an unidentified X-residue at the unphotolyzed state, respectively. The idea for the derivation of the equation has been described previously [164]. (C) Plots of the part of the second H^+-uptake after initial H^+-release as a function of time [162]. All values obtained at varying pH values (◇, pH 7.1; ▽, pH 7.5; △, pH 7.9; □, pH 8.4; ○, pH 9.0) were plotted as relative values. Continuous curves are fitting curves with single exponential eqs. (D) pH dependence of the rate constants of the second H^+-uptake (k_u). Increments of k_u at each pH obtained by subtraction of the minimum value at the highest pH were plotted as relative values. Filled and empty circles represent the plots for BR and ARII, respectively. These plots were well fitted with the Henderson–hasselbalch equation with a single pK_a value. Respective fitting curves for BR and ARII are shown using solid and broken curves. Panels A and B were adapted with permission from Tamogami et al. [164], Biochemistry copyright 2016 American Chemical Society, whereas panels C and D were adapted with permission from Tamogami et al. [162], Photochem. Photobiol. Copyright 2009 the authors, journal compilation, the American Society of Photobiology.*

substitution of $Glu108^{GPR}$ with BR and LR-like aspartate or even ESR-like lysine (data unpublished). Therefore, the distinct mechanisms of CP proton translocation via their proton donors and the specificity of the respective proton donors in the

three types of H^+-pumping rhodopsins may originate from the difference in the environment around each proton donor in the CP channel.

3.6 Existence of two substates in the latter photoproducts of the photocycle and the chemical and structural events occurring during the transition between them

Among the three photointermediates M, N, and O produced in the latter half of the photocycle in H^+-pumping rhodopsins, two spectrally silent substates are known for each photoproduct [33, 132]. Because the transitions between these substates occur without apparent spectral changes, they are usually observed by kinetic analysis for transient absorbance changes measured using various spectroscopic techniques. Three critical events for proton translocation occur during these silent transitions. As is known in BR, the first crucial event was observed upon the transition between two successive M-states, M_1 and M_2, which is accompanied by the accessibility switch of SB from the EC side to the CP side. This switching is important for unidirectional proton transport because it causes the conversion of the direction of proton movement from toward EC at M to toward CP at N.

The second event occurs during the N_1-to-N_2 transition, where the accessibility of the proton donor changes. In BR, the proton donor $Asp96^{BR}$ connects to the SB but not the CP bulk during the M–N transition, thus hampering the misdirected transfer of a proton of $Asp96^{BR}$ toward the CP solvent. Then, the connection of $Asp96^{BR}$ to SB is switched toward the CP side upon the N_1–N_2 transition, facilitating the reprotonation of $Asp96^{BR}$ from the CP surface [33, 45]. Although the detailed mechanism of this accessibility switch upon N_1–N_2 transition remains incompletely understood, even in the most well-known BR, a previous computational study by Wang et al. proposed a model in which the further opening of the proton uptake pathway in the CP channel, which remains closed even in the M-state with the opening of the F-helix by the presence of a hydrophobic barrier composed of $Phe42^{BR}$ and multiple other hydrophobic residues, is triggered by the deprotonation of $Asp96^{BR}$ during the M–N transition, leading to the connection of $Asp96^{BR}$ to the CP aqueous space [155]. In contrast, for the algal H^+-pump ARII, it was presumed that the change in the unique interhelical interaction between $Asp92^{ARII}$ and $Cys218^{ARII}$ located in the CP domain acts as a switch for opening the gate of the CP channel for H^+-uptake [133].

In contrast to M and N, the molecular events in the O-state have not been completely examined because the stable trapping of O produced in the latter stages of the photocycle is difficult. In the early stages of studies on BR, Haupts et al. hypothesized that during the N–O transition, the reisomerization of the retinal from the 13-*cis* (15-*anti* PSB) to all-*trans* (15-*syn* PSB) form is followed by the switching of the N-H bond of PSB from the CP (15-*syn* PSB) to the EC (15-*anti* PSB) side, the so-called isomerization/switch/transfer (IST) model [156]. In contrast, the results of MD simulation performed by Wang et al. supported the opposite model (SIT model) as a more plausible scheme: the isomerization of the retinal from 13-*cis* (15-*syn* PSB) to all-*trans* (15-*anti* PSB) is preceded by the switching of PSB from the 15-*anti* to 15-*syn* forms [157]. If the scheme corresponds to the latter model, another substate with a 13-*cis* chromophore should be formed after the switching of PSB during the N_2-O transition with the thermal reisomerization of retinal. Thus, we attempted to detect the presence of further substates. In general, the existence of the quasi-equilibrium among M, N, and O states described above makes it difficult to observe O. However, in the algal H^+-pump ARII under acidic conditions (pH $< \sim$5.5), N did not accumulate during the photocycle due to the presence of a rapid

back reaction between M and N and the acceleration of proton uptake upon the following N–O transition under these conditions, resulting in notable observation of O [132]. Through kinetic analysis of time-resolved absorbance changes under these conditions, we succeeded in detecting two spectral analogous O-intermediates (O_1 and O_2) [132]. As the O_1–O_2 transition was accompanied by a faint but obvious red-shift of the absorption maximum, we assumed that the 13-*cis*-to-all-*trans* retinal isomerization occurs during the O_1–O_2 transition after the switching of PSB upon the N_2–O_1 transition based on the model proposed by Wang et al. [157]: O_1 is a precursor before the formation of O (O_2) with a twisted all-*trans* chromophore retinal. In previous studies on BR, it was reported that the steric contact of $Lue93^{BR}$ with the 13-methyl group of retinal is significant for facilitated retinal reisomerization during this transition [158]. The residue corresponding to this leucine is almost completely conserved among all microbial rhodopsins (see **Figure 2**), implying that the mechanism described above is common in the microbial rhodopsin family.

3.7 Role of PRC formed on the EC surface

As described above, PRC located on the EC surface is not necessarily indispensable for proton pumping because of the presence of a PRC-deficient type (eubacterial or eukaryotic) H^+-pumping rhodopsins, although PRC alters the timing of proton release during the photocycle. The replacement of either $Glu194^{BR}$, $Glu204^{BR}$, or both by nonionizable residues, however, caused a delay in O-decay with a late proton release from the protonated $Asp85^{BR}$ toward the EC surface as well as the absence of the initial proton release upon the L–M transition. In addition, when the residues corresponding to three of PRC-constituting residues ($Ser193^{BR}$, $Glu194^{BR}$, and $Thr205^{BR}$) in a sensory-type rhodopsin from *Natronomonas pharaonis* (NpSRII) were replaced by the same residues as BR, the lifetime of O in this triple NpSRII mutant became approximately 20-fold shorter than that of the wild type [159]. Hence, the presence of PRC on the EC surface may be involved in not only the early proton release toward the EC aqueous phase during the photocycle but also in the formation of a hydrophilic proton conductive pathway in the EC channel, which contributes to efficient proton translocation. In contrast, as observed in the X-ray crystal structure of ESR, there may be a cavity for the proton releasing pathway that already connects to the EC bulk solvent at the resting state in eubacterial H^+-pumping rhodopsins without PRC. Thus, in the EC domain of these H^+-pumping rhodopsins, a hydrophilic pathway may be formed in a different manner from archaeal H^+-pumps, participating in facilitated proton movement on the EC side.

3.8 Importance of the method for pK_a estimation of crucial residues involved in proton transfer

As described previously, sequential proton transfer events during the photocycles in various microbial H^+-pumping rhodopsins, including BR, are successfully accomplished by regulating rigorous pK_a changes among the crucial residues (particularly, PSB (or deprotonated SB), its proton acceptor, donor, and known or unknown proton-releasing residue(s)) related to proton translocation. The estimation of the pK_a values of these residues in both unphotolyzed and photolyzed states, therefore, provides important clues for understanding the proton transfer mechanism in these H^+-pumps. Such pK_a values can be indirectly estimated using spectroscopic approaches, such as FTIR or NMR. However, the establishment of a more direct method for pK_a estimation is preferable, which can be achieved by

measuring the photoinduced proton exchange between the protein and media (proton uptake/release) arising as a result of proton transfer events during the photocycle at varying pH values.

As a method for measuring proton movement transiently occurring during the photocycles of these pigments, the conventional method of using various pH-indicator dyes is frequently employed [44]. This method is highly time-resolved because the transient pH changes of the media with photoinduced proton uptake and release in rhodopsins are monitored based on the real-time transient absorbance changes of these pH-sensitive dyes in the sample suspension. The use of this method, therefore, enables us to precisely identify the timing of proton uptake and release together with the rise and decay kinetics of photoproducts. However, the pH range for measurement is confined to the pH values around its pK_a; therefore, pK_a estimation using this method is difficult. In contrast, another method using a tin oxide (SnO_2 or indium-tin oxide, ITO) transparent electrode [160–163] is also highly pH-sensitive and rapidly time-resolved, although the applicable time period is limited within the time scale from several ten to hundred microseconds to hundreds of milliseconds [162, 164]. Moreover, this method can detect small pH changes with photoinduced proton uptake and release in the vicinity of a protein-attached electrode as a sufficiently large amplitude of voltage changes, even in solutions containing a small amount of buffer agents. Based on these advantages, we applied this method to the pK_a estimation in H^+-pumps from three biological kingdoms, BR, GPR, and ARII [130, 162, 164]. The pK_a estimation was performed in two ways. One method estimates the pK_a value from the pH dependence of the magnitude of voltage changes, reflecting proton uptake and release. **Figure 3A** shows the photoinduced transient proton transfers in GPR at varying pH values, where the upward and downward shifts represent proton release and uptake, respectively. Because the peak time and magnitude of these data depend on both the on- and off-time constants, the fraction of the subpopulation inducing proton uptake or release at the respective pH values is estimated by fitting with the kinetically derived theoretical equation. **Figure 3B** shows the plots of the values estimated from the above fitting analysis as a function of pH. From further fitting analysis for these plots with an equation developed based on the Henderson–Hasselbalch theory, we succeeded in estimating the pK_a values of some residues associated with photoinduced proton transfer events in GPR [164]. In contrast, the direct plots of amplitudes of light-induced proton transfer signals without strict regression described above, which are approximately proportional to the amount of proton transfer, also exhibited similar pH-dependent behavior, although these plots include some error. Therefore, such plotting may be useful as a method for simply estimating the approximate pK_a values. Another method estimates the pK_a values from the pH dependence of the kinetics of photoinduced proton uptake or release. **Figure 3C** shows the pH-dependent changes in the traces of the part representing the latter proton uptake following the initial release of a proton in BR in the pH range of 6.5 9.5. The fitting for these traces with a single exponential equation (solid curves in this figure) gave the rate constant values of proton uptake at the respective pH values. Similarly, the estimated values of the rate constant at each pH were plotted against pH (**Figure 3D**), and sequentially, the pK_a values of $Asp96^{BR}$ in H^+-uptake (N-O transition) were estimated using the Henderson–Hasselbalch Equation [162]. All other BR values estimated by these methods were consistent with the corresponding values previously estimated using other experimental approaches [45] (also see **Figure 4B**). Therefore, this method for estimating the pK_a values of some crucial residues for proton pumping, which is an index of proton pumping efficiency, may be a powerful and effective tool for screening efficient H^+-pumps or their engineered mutants for optogenetics.

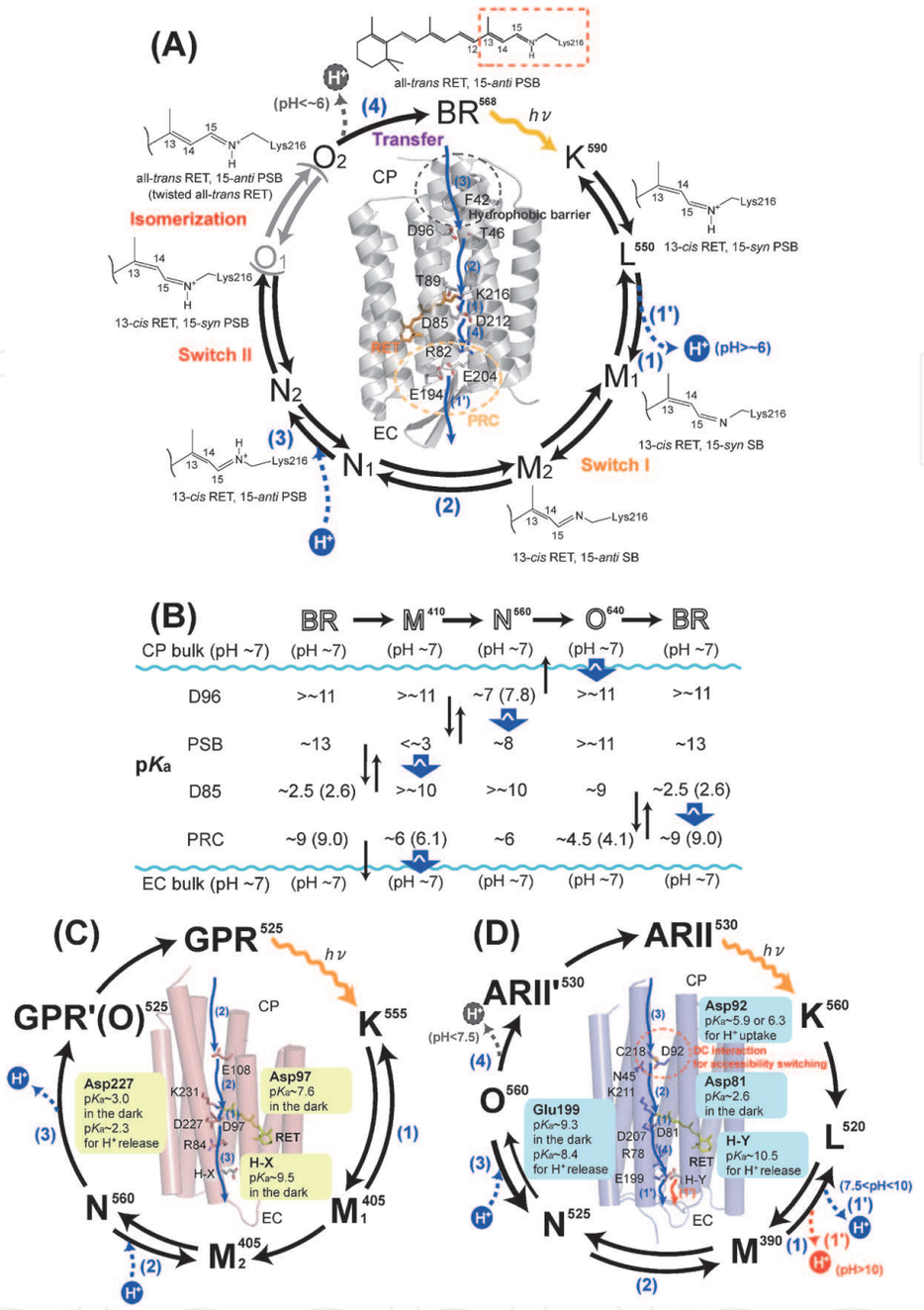

Figure 4.

Schematic representation of the photocycle and accompanying proton transfer of three types of H^+-pumping rhodopsins. (A) Schematic diagram of the photochemistry of BR. The stepwise proton transfer reactions are depicted by thin blue arrows and overlaid on the crystal structure of BR at the dark state (PDB 1c3w). The timing of H^+-release differs depending on pH values. The expected configuration changes of chromophore retinal (RET) and PSB in each photocycle intermediate are also depicted. (B) Summary of pK_a changes in the residues participating in the proton transfer reactions during the photocycle. A transient pK_a increase and decrease of respective residues upon each transition are shown in upward and downward thin arrows. The reverse of pK_a values between two adjacent residues leads to a unidirectional proton movement from a (protonated) residue with a lowered pK_a value to another (unprotonated) residue with an elevated pK_a value. Such proton migrations are expressed in thick blue arrows. The values in parentheses represent our previous estimated pK_a values by the SnO_2 electrode method [162]. (C) Schematic diagram of the photochemistry of a eubacterial H^+-pump GPR. The proton transfer reactions are the case in the pH region below ca. 9.5. H-X represents an unidentified residue whose deprotonation at the initial state induces the formation of another parallel photocycle via a different M-like state (M_a) from normal M and early proton release [164]. (D) Schematic diagram of the photochemistry of a eukaryotic H^+-pump ARII. The timing of H^+-release is divided into three patterns depending on pH [130]: 1) an initial H^+-release from an unknown Y-residue (H-Y) at pH > ~10 (shown in orange arrow), 2) an initial H^+-release from $Glu199^{ARII}$ at ~ 7.5 < pH < ~10 (shown in blue arrow), and 3) a probably direct H^+-release from $Asp81^{ARII}$ at the latter stage (O-ARII' transition) of the photocycle (shown in gray arrow). In panels C and D, the pK_a values of several crucial residues for H^+-pumping in respective rhodopsins, which were previously estimated using the SnO_2 (or ITO) electrode method [130, 145, 164], are shown together.

4. Future perspectives of H^+-pumping rhodopsins as optogenetic tools

As described at the beginning of this chapter, outward H^+-pumping microbial rhodopsins can evoke stronger light-induced neural suppression and quicker recovery from the inactivated state formed upon illumination than inward Cl^--pump HRs. Hence, optical neural control using H^+-pumping rhodopsins may also be an effective alternative for optogenetics, although neural inhibition with light-gated anion channel ACRs has recently attracted attention. The rational design based on the functional molecular basis of these rhodopsins described in this chapter may allow the creation of "neo-type" H^+-pumping microbial rhodopsins by introducing several mutations to further enhance the effect of neural silencing upon illumination, resulting in the acceleration of the development of more efficient tools for optogenetics along with developing color variants with various spectral properties. Further increases in protein expression and stability in targeted neural cells could also lead to the improvement of optogenetic tools. For this purpose, taking advantage of the abundance of these H^+-pumping rhodopsins, the exploration of new microbial H^+-pumping rhodopsins with novel properties (e.g., high thermal stability [165, 166]) from nature may be useful for producing mutants.

In addition, studies on H^+-pumping microbial rhodopsins are required to develop novel optical cellular control methods because these types of pigments can simultaneously induce alkalization of the intracellular pH by illumination-induced outward proton transport. As is generally known, the maintenance of an appropriate cellular pH is necessary to ensure that each requisite enzyme for various biological reactions functions properly. Because the drainage of acids produced by cellular metabolism is controlled through the Na^+/H^+ antiporter or the Cl^-/HCO_3^- exchanger to maintain the cellular pH near neutral, failure in these transporting systems affects the normal function of cells. Therefore, the application of optogenetics to cells with abnormal pH values, that is, light-induced manipulation of the cells specifically expressing H^+-pumping microbial rhodopsins, may allow the restoration of the functions of these cells. As an example of intracellular pH regulation by optogenetics, Matsui et al. reported that the photoinduced intracellular pH increase in glial cells expressing aR-3 (Arch) suppressed the release of glutamate from these cells, which was triggered by glial acidosis upon brain ischemia, thereby ameliorating the effects of ischemic brain damage [167]. Moreover, the optical regulation of the function of varying organelles expressing H^+-pumping rhodopsins has recently been attempted. Rost et al. demonstrated that selective Arch expression on synaptic vesicles together with a pH-sensitive indicator and successive illumination led to vesicular acidification via Arch instead of vacuolar-type H^+-ATPases (V-ATPases), enabling neurotransmitter accumulation within synaptic vesicles driven by the proton motive force (PMF) generated through light-activated Arch [168]. In addition, Hara et al. achieved dR-2-mediated optical partial suppression of cell death induced by the inhibition of respiratory PMF generation in the mitochondria of mammalian cells [169]. More recently, a method for topological inversion of microbial rhodopsins as optogenetic tools was also developed [170]. Hence, the application of this technique together with the use of recently discovered natural inward H^+-pumping rhodopsins [171, 172] as optogenetic tools may allow the induction of both light-activated acidification and alkalization in various types of cells or organelles such as mitochondria, vesicles, and lysosomes. Hence, the combination of an outward H^+-pumping rhodopsin and the topological reversal technique described above may allow various types of optogenetics. For instance, the use of outward H^+-pumping rhodopsin might lead to the following optogenetics: in general, the pH values of lysosomes in normal cells are regulated to be approximately 5, whereas those of lysosomes in cancer cells with acquired resistance to

carcinostatic agents tend to be lower [173, 174]. The efficacy of carcinostatic agents for these cancer cells is degraded because they get trapped in acidified organelles; therefore, specific expression of H^+-pumping rhodopsins in lysosomes of drug-resistant cancer cells and optical pH control (photoinduced alkalization) of these cellular organelles might lead to the restoration of the original effect of drugs. Thus, optogenetics using H^+-pumping microbial rhodopsins may lead to the establishment of new optical therapies in the future.

5. Conclusion

Proton pump-type microbial rhodopsins are not only effective neural suppressors but also optical tools for pH control of various cells or organelles that specifically incorporate these pigments, which makes them a dual optogenetic tool. Rational protein engineering based on molecular mechanisms is required to further develop these rhodopsins into more effective tools. Considering the photochemical reaction and accompanying proton transfer mechanism in various H^+-pumping rhodopsins described previously, mutations that increase their photocycle kinetics may be effective for enhancing the respective H^+-pumping abilities. To increase their H^+-pumping efficiency via their photocycles, for example, a mutation that lowers the pK_a values of proton acceptors in the unphotolyzed state, which increases the population with H^+-pumping activity, may be effective. Alternatively, alterations that lead to a reduction in the pK_a of the proton donor upon M–N transition (donor-to-SB H^+-transfer) and to an increase in its pK_a value upon N–O transition (H^+-uptake) may be efficacious for promoting CP-side proton transfer. In addition, the introduction of PRC-forming residues on the EC surface may facilitate EC proton transfer. While screening for more effective tools among such designed mutants based on their molecular mechanism, the SnO_2 (ITO) electrode method could be a simple and efficient tool for estimating the pK_a values of critical residues for proton pumps, which is an index of proton pumping effectiveness. Thus, through a series of investigations on H^+-pumping rhodopsins based on molecular mechanisms, novel optogenetic H^+-pumping rhodopsins could be developed in the near future.

Conflict of interest

The authors declare no competing financial interests.

DOI: http://dx.doi.org/10.5772/intechopen.97589

Author details

Jun Tamogami[1*] and Takashi Kikukawa[2]

1 College of Pharmaceutical Sciences, Matsuyama University, Matsuyama, Ehime, Japan

2 Faculty of Advanced Life Science, Hokkaido University, Sapporo, Japan

*Address all correspondence to: jtamoga@g.matsuyama-u.ac.jp

References

[1] Boyden ES, Zhang F, Bamberg E, Nagel G, Deisseroth K. Millisecond-timescale, genetically targeted optical control of neural activity. Nature Neuroscience. 2005;**8**:1263-1268.

[2] Nagel G, Brauner M, Liewald JF, Adeishvili N, Bamberg E, Gottschalk A. Light activation of channelrhodopsin-2 in excitable cells of *Caenorhabditis elegans* triggers rapid behavioral responses. Current Biology. 2005;**15**: 2279-2284. DOI: 10.1016/j.cub.2005.11.032

[3] Zhang F, Wang LP, Boyden ES, Deisseroth K. Channelrhodopsin-2 and optical control of excitable cells. Nature Methods. 2006;**3**:785-792. DOI: 10.1038/NMETH936

[4] Zhang F, Wang LP, Brauner M, Liewald JF, Kay K, Watzke N, Wood PG, Bamberg E, Nagel G, Gottschalk A, Deisseroth K. Multimodal fast optical interrogation of neural circuitry. Nature. 2007;**446**:633-639. DOI: 10.1038/nature05744

[5] Zhang F, Aravanis AM, Adamantidis A, de Lecea L, Deisseroth, K. Circuit-breakers: optical technologies for probing neural signals and systems. Nature Reviews Neuroscience. 2007;**8**: 577-581. DOI: 10.1038/nrn2192

[6] Häusser M, Smith SL. Controlling neural circuits with light. Nature. 2007; **446**:617-619. DOI: 10.1038/446617a

[7] Han X, Qian X, Bernstein JG, Zhou HH, Franzesi GT, Stern P, Bronson RT, Graybiel AM, Desimone R, Boyden ES. Millisecond-timescale optical control of neural dynamics in the nonhuman primate brain. Neuron. 2009;**62**:191-198. DOI: 10.1016/j.neuron.2009.03.011

[8] Deisseroth K, Hegemann P. The form and function of channelrhodopsin. Science. 2017;**357**:eaan5544. DOI: 10.1126/science.aan5544

[9] Gradinaru V, Zhang F, Ramakrishnan C, Mattis J, Prakash R, Diester I, Goshen I, Thompson KR, Deisseroth K. Molecular and cellular approaches for diversifying and extending optogenetics. Cell. 2010;**141**: 154-165. DOI: 10.1016/j.cell.2010.02.037

[10] Kleinlogel S, Feldbauer K, Dempski RE, Fotis H, Wood PG, Bamann C, Bamberg E. Ultra light-sensitive and fast neuronal activation with the Ca^{2+}-permeable channelrhodopsin CatCh. Nature Neuroscience. 2011;**14**:513-518. DOI: 10.1038/nn.2776

[11] Wietek J, Wiegert JS, Adeishvili N, Schneider F, Watanabe H, Tsunoda SP, Vogt A, Elstner M, Oertner TG, Hegemann P. Conversion of channelrhodopsin into a light-gated chloride channel. Science. 2014;**344**: 409-412. DOI: 10.1126/science.1249375

[12] Bedbrook CN, Yang KK, Robinson JE, Mackey ED, Gradinaru V, Arnold FH. Machine learning-guided channelrhodopsin engineering enables minimally-invasive optogenetics. Nature Methods. 2019;**16**: 1176-1184. DOI: 10.1038/s41592-019-0583-8

[13] Cho YK, Park D, Yang A, Chen F, Chuong AS, Klapoetke NC, Boyden ES. Multidimensional screening yields channelrhodopsin variants having improved photocurrent and order-of-magnitude reductions in calcium and proton currents. The Journal of Biological Chemistry. 2019;**294**: 3806-3821. DOI: 10.1074/jbc.RA118.006996

[14] Oppermann J, Fischer P, Silapetere A, Liepe B, Rodriguez-Rozada S, Flores-Uribe J, Peter E, Keidel A,

Vierock J, Kaufmann J, Broser M, Luck M, Bartl F, Hildebrandt P, Wiegert JS, Béjà O, Hegemann P, Wietek J. MerMAIDs: a family of metagenomically discovered marine anion-conducting and intensely desensitizing channelrhodopsins. Nature Communications. 2019;**10**:3315. DOI: 10.1038/s41467-019-11322-6

[15] Li X, Gutierrez DV, Hanson MG, Han J, Mark MD, Chiel H, Hegemann P, Landmesser LT, Herlitze S. Fast noninvasive activation and inhibition of neural and network activity by vertebrate rhodopsin and green algae channelrhodopsin. Proceedings of the National Academy of Sciences of the United States of America. 2005;**102**: 17816-17821. DOI: 10.1073_ pnas.0509030102

[16] Levskaya A, Weiner OD, Lim WA, Voigt CA. Spatiotemporal control of cell signalling using a light-switchable protein interaction. Nature. 2009;**461**: 997-1001. DOI: 10.1038/nature08446

[17] Sierra YAB, Rost BR, Pofahl M, Fernandes AM, Kopton RA, Moser S, Holtkamp D, Masala N, Beed P, Tukker JJ, Oldani S, Bönigk W, Kohl P, Baier H, Schneider-Warme F, Hegemann P, Beck H, Seifert R, Schmitz D. Potassium channel-based optogenetic silencing. Nature Communications. 2018;**9**:4611. DOI: 10.1038/s41467-018-07038-8

[18] Bamann C, Nagel G, Bamberg E. Microbial rhodopsins in the spotlight. Current Opinion in Neurobiology. 2010; **20**:610-616. DOI: 10.1016/j. conb.2010.07.003

[19] Zhang F, Vierock J, Yizhar O, Fenno LE, Tsunoda S, Kianianmomeni A, Prigge M, Berndt A, Cushman J, Polle J, Magnuson J, Hegemann P, Deisseroth K. The microbial opsin family of optogenetic tools. Cell. 2011;**147**:1446-1457. DOI 10.1016/j.cell.2011.12.004

[20] Spudich JL, Yang CS, Jung KH, Spudich EN. Retinylidene proteins: structures and functions from archaea to humans. Annual Review of Cell and Developmental Biology. 2000;**16**: 365-392. DOI: 10.1146/annurev. cellbio.16.1.365

[21] Béjà O, Lanyi JK. Nature's toolkit for microbial rhodopsin ion pumps. Proceedings of the National Academy of Sciences of the United States of America. 2014;**111**: 6538-6539. DOI: 10.1073/pnas.1405093111

[22] Ernst OP, Lodowski DT, Elstner M, Hegemann P, Brown LS, Kandori H. Microbial and animal rhodopsins: structures, functions, and molecular mechanisms. Chemical Reviews. 2014; **114**:126-163. DOI: 10.1021/cr4003769

[23] Grote M, Engelhard M, Hegemann P. Of ion pumps, sensors and channels — Perspectives on microbial rhodopsins between science and history. Biochimica et Biophysica Acta. 2014; **1837**:533-545. DOI: 10.1016/j. bbabio.2013.08.006

[24] Inoue K, Kato Y, Kandori H. Light-driven ion-translocating rhodopsins in marine bacteria. Trends in Microbiology. 2015;**23**:91-98. DOI: 10.1016/j.tim.2014.10.009

[25] Nagel G, Ollig D, Fuhrmann M, Kateriya S, Musti AM, Bamberg E, Hegemann P. Channelrhodopsin-1: a light-gated proton channel in green algae. Science. 2002;**296**:2395-2398. DOI: 10.1126/science.1072068

[26] Nagel G, Szellas T, Huhn W, Kateriya S, Adeishvili N, Berthold P, Ollig D, Hegemann P, Bamberg E. Channelrhodopsin-2, a directly light-gated cation-selective membrane channel. Proceedings of the National Academy of Sciences of the United States of America. 2003;**100**: 13940-13945. DOI: 10.1073_ pnas.1936192100

[27] Nagel G, Szellas T, Kateriya S, Adeishvili N, Hegemann P, Bamberg E. Channelrhodopsins: directly light-gated cation channels. Biochemical Society Transactions. 2005;**33**:863-866. DOI: 10.1042/BST0330863

[28] Govorunova EG, Sineshchekov OA, Janz R, Liu X, Spudich JL. Natural light-gated anion channels: a family of microbial rhodopsins for advanced optogenetics. Science. 2015;**349**: 647-650. DOI: 10.1126/science.aaa7484

[29] Govorunova EG, Sineshchekov OA, Spudich JL. *Proteomonas sulcata* ACR1: a fast anion channelrhodopsin. Photochemistry and Photobiology. 2016;**92**:257-263. DOI: 10.1111/php.12558

[30] Govorunovaa EG, Sineshchekova OA, Lia H, Wanga Y, Brownb LS, Spudicha JL. RubyACRs, nonalgal anion channelrhodopsins with highly red-shifted absorption. Proceedings of the National Academy of Sciences of the United States of America. 2020;**117**:22833-22840. DOI: 10.1073/pnas.2005981117

[31] Govorunova EG, Sineshchekov OA, Hemmati R, Janz R, Morelle O, Melkonian M, Wong GKS, Spudich JL. Extending the time domain of neuronal silencing with cryptophyte anion channelrhodopsins. eNeuro. 2018;**5**: ENEURO.0174-18.2018. DOI: 10.1523/ENEURO.0174-18.2018

[32] Haupts U, Tittor J, Oesterhelt D. Closing in on bacterorhodopsin: progress in understanding the molecule. Annual Review of Biophysics and Biomolecular Structure. 1999;**28**: 367-399. DOI: 10.1146/annurev.biophys.28.1.367

[33] Lanyi JK. Bacteriorhodopsin. Annual Review of Physiology. 2004;**66**: 665-688. DOI: 10.1146/annurev.physiol.66.032102.150049

[34] Inoue K, Ono H, Abe-Yoshizumi R, Yoshizawa S, Ito H, Kogure K, Kandori H. A light-driven sodium ion pump in marine bacteria. Nature Communications. 2013;**4**:1678. DOI: 10.1038/ncomms2689

[35] Mukohata Y, Ihara K, Tamura T, Sugiyama Y. Halobacterial rhodopsins. The Journal of Biochemistry. 1999;**125**: 649-657. DOI: 10.1093/oxfordjournals.jbchem.a022332

[36] Váró G. Analogies between halorhodopsin and bacteriorhodopsin. Biochimica et Biophysica Acta. 2000; **1460**:220-229. DOI: 10.1016/S0005-2728(00)00141-9

[37] Essen LO. Halorhodopsin: light-driven ion pumping made simple? Current Opinion in Structural Biology. 2002;**12**:516-522. DOI: 10.1016/S0959-440X(02)00356-1

[38] Engelhard C, Chizhov I, Siebert F, Engelhard M. Microbial halorhodopsins: light-driven chloride pumps. Chemical Reviews. 2018;**118**:10629-10645. DOI: 10.1021/acs.chemrev.7b00715

[39] Chow BY, Han X, Dobry AS, Qian X, Chuong AS, Li M, Henninger MA, Belfort GM, Lin Y, Monahan PE, Boyden ES. High-performance genetically targetable optical neural silencing by light-driven proton pumps. Nature. 2010;**463**: 98-102. DOI: 10.1038/nature08652

[40] Grimm C, Silapetere A, Vogt A, Bernal Sierra YA, Hegemann P. Electrical properties, substrate specificity and optogenetic potential of the engineered light-driven sodium pump eKR2. Scientific Reports. 2018; **8**:9316. DOI: 10.1038/s41598-018-27690-w

[41] Finkel OM, Béjà O, Belkin S. Global abundance of microbial rhodopsins. The ISME Journal. 2013;**7**:448-451. DOI: 10.1038/ismej.2012.112

[42] Oesterhelt D, Stoeckenius W. Rhodopsin-like Protein from the Purple Membrane of *Halobacterium halobium*. Nature New Biology. 1971;**233**:149-152. DOI: 10.1038/newbio233149a0

[43] Subramaniam S. The structure of bacteriorhodopsin: an emerging consensus. Current Opinion in Structural Biology. 1999;**9**:462-468. DOI: 10.1016/S0959-440X(99)80065-7

[44] Heberle J. Proton transfer reactions across bacteriorhodopsin and along the membrane. Biochimica et Biophysica Acta. 2000;**1458**:135-147. DOI: 10.1016/s0005-2728(00)00064-5

[45] Balashov SP. Protonation reactions and their coupling in bacteriorhodopsin. Biochimica et Biophysica Acta. 2000; **1460**:75-94. DOI: 10.1016/s0005-2728 (00)00131-6

[46] Subramaniam S, Henderson R. Crystallographic analysis of protein conf ormational changes in the bacteriorhod opsin photocycle. Biochimica et Biophysica Acta. 2000;**1460**:157-165. DOI: 10.1016/s0005-2728(00)00136-5

[47] Kandori H. Role of internal water molecules in bacteriorhodopsin. Biochimica et Biophysica Acta. 2000; **1460**:177-191. DOI: 10.1016/s0005-2728 (00)00138-9

[48] Wickstrand C, Nogly P, Nango E, Iwata S, Standfuss J, Neutze R. Bacteriorhodopsin: structural insights revealed using X-ray lasers and synchrotron radiation. Annual Review of Biochemistry. 2019;**88**:59-83. DOI: 10.1146/annurev-biochem-013118-111327

[49] Mukohata Y, Sugiyama Y, Ihara K, Yoshida M. An Australian halobacterium contains a novel proton pump retinal protein: archaerhodopsin. Biochemical and Biophysical Research Communications. 1988;**151**:1339-1345. DOI: 10.1016/S0006-291X(88)80509-6

[50] Ihara K, Umemura T, Katagiri I, Kitajima-Ihara T, Sugiyama Y, Kimura Y, Mukohata Y. Evolution of the archaeal rhodopsins: evolution rate changes by gene duplication and functional differentiation. Journal of Molecular Biology. 1999;**285**:163-174. DOI: 10.1006/jmbi.1998.2286

[51] Li Q, Sun Q, Zhao W, Wang H, Xu D. Newly isolated archaerhodopsin from a strain of Chinese halobacteria and its proton pumping behavior. Biochimica et Biophysica Acta. 2000; **1466**:260-266. DOI: 10.1016/ S0005-2736(00)00188-7

[52] Chaoluomeng, Dai G, Kikukawa T, Ihara K, Iwasa T (2015). Microbial rhodopsins of *Halorubrum* species isolated from Ejinoor salt lake in Inner Mongolia of China. Photochemical & Photobiological Sciences. 2015;**14**: 1974-82. DOI: 10.1039/c5pp00161g

[53] Geng X, Dai G, Chao L, Wen D, Kikukawa T, Iwasa T. Two consecutive polar amino acids at the end of helix E are important for fast turnover of the archaerhodopsin photocycle. Photochemistry and Photobiology. 2019;**95**:980-989. DOI: 10.1111/ php.13072

[54] Tateno M, Ihara K, Mukohata Y. The novel ion pump rhodopsins from *Haloarcula* form a family independent from both the bacteriorhodopsin and archaerhodopsin families/tribes. Archives of Biochemistry and Biophysics. 1994;**315**:127-132. DOI: 10.1006/abbi.1994.1480

[55] Sugiyama Y, Yamada N, Mukohata Y. The light-driven proton pump, cruxrhodopsin-2 in *Haloarcula* sp. arg-2 (bR^+, hR^-), and its coupled ATP formation. Biochimica et Biophysica Acta. 1994;**1188**:287-292. DOI: 10.1016/0005-2728(94)90047-7

[56] Kitajima T, Hirayama J, Ihara K, Sugiyama Y, Kamo N. Novel bacterial

rhodopsins from *Haloarcula vallismortis*. Biochemical and Biophysical Research Communications. 1996;**345**:341-345. DOI: 10.1006/bbrc.1996.0407

[57] Kamekura M, Seno Y, Tomioka H. Detection and expression of a gene encoding a new bacteriorhodopsin from an extreme halophile strain HT (JCM 9743) which does not possess bacteriorhodopsin activity. Extremophiles. 1998;**2**:33-39. DOI: 10.1007/s007920050040

[58] Brown LS, Jung KH. Bacteriorhodopsin-like proteins of eubacteria and fungi: the extent of conservation of the haloarchaeal proton-pumping mechanism. Photochemical & Photobiological Sciences. 2006;**5**: 538-546. DOI: 10.1039/b514537f

[59] Brown LS. Eubacterial rhodopsins — Unique photosensors and diverse ion pumps. Biochimica et Biophysica Acta. 2014;**1837**:553-561. DOI: 10.1016/j.bbabio.2013.05.006

[60] Fuhrman JA, Schwalbach MS, Stingl U. Proteorhodopsins: an array of physiological roles? Nature Reviews Mic robiology. 2008;**6**:488-494. DOI: 10.1038/nrmicro1893

[61] Bamann C, Bamberg E, Wachtveitl J, Glaubitz C. Proteorhodopsin. Biochimica et Biophysica Acta. 2014;**1837**:614-625. DOI: 10.1016/j.bbabio.2013.09.010

[62] Béjà O, Aravind L, Koonin EV, Suzuki MT, Hadd A, Nguyen LP, Jovanovich SB, Gates CM, Feldman RA, Spudich JL, Spudich EN, DeLong EF. Bacterial rhodopsin: evidence for a new type of phototrophy in the Sea. Science. 2000;**289**:1902-1906. DOI: 10.1126/science.289.5486.1902

[63] Giovannoni SJ, Bibbs L, Cho JC, Stapels MD, Desiderio R, Vergin KL, Rappé MS, Laney S, Wilhelm LJ, Tripp HJ, Mathur EJ, Barofsky DF. Proteorhodopsin in the ubiquitous marine bacterium SAR11. Nature. 2005; **438**:82-85. DOI: 10.1038/nature04032

[64] Courties A, Riedel T, Jarek M, Intertaglia L, Lebaron P, Suzuki MT. Genome sequence of strain MOLA814, a proteorhodopsin-containing representative of the *Betaproteobacteria* common in the ocean. Genome Announcements. 2013;**1**:e01062-e01013. DOI: 10.1128/genomeA.01062-13

[65] Gómez-Consarnau L, González JM, Coll-Lladó M, Gourdon P, Pascher T, Neutze R, Pedrós-Alió C, Pinhassi J. Light stimulates growth of proteorhodopsin-containing marine Flavobacteria. Nature. 2007;**445**: 210-213. DOI: 10.1038/nature05381

[66] Zhao M, Chen F, Jiao N. Genetic diversity and abundance of Flavobacterial proteorhodopsin in China Seas. Applied and Environmental Microbiology. 2009;**75**:529-533. DOI: 10.1128/AEM.01114-08

[67] Béjà O, Spudich EN, Spudich JL, Leclerc M, DeLong EF. Proteorhodopsin phototrophy in the ocean. Nature. 2001; **411**:786-789. DOI: 10.1038/35081051

[68] Sabehi G, Massana R, Bielawski JP, Rosenberg M, Delong EF, Béjà O. Novel proteorhodopsin variants from the Mediterranean and Red Seas. Environmental Microbiology. 2003;**5:** 842-849. DOI: 10.1046/j.1462-2920.2003.00493.x

[69] de la Torre JR, Christianson LM, Béjà O, Suzuki MT, Karl DM, Heidelberg J, DeLong EF. Proteorhodopsin genes are distributed among divergent marine bacterial taxa. Proceedings of the National Academy of Sciences of the United States of America. 2003;**100**:12830-12835. DOI: 10.1073_pnas.2133554100

[70] Venter JC, Remington K, Heidelberg JF, Halpern AL, Rusch D,

Eisen JA, Wu D, Paulsen I, Nelson KE, Nelson W, Fouts DE, Levy S, Knap AH, Lomas MW, Nealson K, White O, Peterson J, Hoffman J, Parsons R, Baden-Tillson H, Pfannkoch C, Rogers YH, Smith HO. Environmental genome shotgun sequencing of the Sargasso Sea. Science. 2004;**304**:66-74. DOI: 10.1126/science.1093857

[71] Rusch DB, Halpern AL, Sutton G, Heidelberg KB, Williamson S, Yooseph S, Wu D, Eisen JA, Hoffman JM, Remington K, Beeson K, Tran B, Smith H, Baden-Tillson H, Stewart C, Thorpe J, Freeman J, Andrews-Pfannkoch C, Venter JE, Li K, Kravitz S, Heidelberg JF, Utterback T, Rogers YH, Falcón LI, Souza V, Bonilla-Rosso G, Eguiarte LE, Karl DM, Sathyendranath S, Platt T, Bermingham E, Gallardo V, Tamayo-Castillo G, Ferrari MR, Strausberg RL, Nealson K, Friedman R, Frazier M, Venter JC. The sorcerer II global ocean sampling expedition: northwest Atlantic through eastern tropical Pacific. PLoS Biology. 2007;**5**:e77. DOI: 10.1371/journal.pbio.0050077

[72] Yoshizawa S, Kawanabe A, Ito H, Kandori H, Kogure K. Diversity and functional analysis of proteorhodopsin in marine *Flavobacteria*. Environmental Microbiology. 2012;**14**:1240-1248. DOI: 10.1111/j.1462-2920.2012.02702.x

[73] Man D, Wang W, Sabehi G, Aravind L, Post AF, Massana R, Spudich EN, Spudich JL, Béjà O. Diversification and spectral tuning in marine proteorhodopsins. The EMBO Journal. 2003;**22**:1725-1731. DOI: 10.1093/emboj/cdg183

[74] Bielawski JP, Dunn KA, Sabehi G, Béjà O. Darwinian adaptation of proteorhodopsin to different light intensities in the marine environment. Proceedings of the National Academy of Sciences of the United States of America. 2004;**101**:14824-14829. DOI: 10.1073_pnas.0403999101

[75] Sabehi G, Kirkup BC, Rozenberg M, Stambler N, Polz MF, Béjà O. Adaptation and spectral tuning in divergent marine proteorhodopsins from the eastern Mediterranean and the Sargasso Seas. The ISME Journal. 2007;**1**: 48-55. DOI: 10.1038/ismej.2007.10

[76] Sharma AK, Zhaxybayeva O, Papke RT, Doolittle WF. Actinorhodopsins: proteorhodopsin-like gene sequences found predominantly in non-marine environments. Environmental Microbiology. 2008;**10**: 1039-1056. DOI:10.1111/j.1462-2920.2007.01525.x

[77] Bohorquez LC, Ruiz-Perez CA, Zambrano MM. Proteorhodopsin-like genes present in thermoacidophilic high-mountain microbial communities. Applied and Environmental Microbiology. 2012;**78**:7813-7817. DOI: 10.1128/AEM.01683-12

[78] Murugapiran SK, Huntemann M, Wei CL, Han J, Detter JC, Han CS, Erkkila TH, Teshima H, Chen A, Kyrpides N, Mavrommatis K, Markowitz V, Szeto E, Ivanova N, Pagani I, Lam J, McDonald AI, Dodsworth JA, Pati A, Goodwin L, Peters L, Pitluck S, Woyke T, Hedlund BP. Whole genome sequencing of *Thermus oshimai* JL-2 and *Thermus thermophilus* JL-18, incomplete denitrifiers from the United States Great Basin. Genome Announcements. 2013;**1**: e00106-e00112. DOI: 10.1128/genomeA.00106-12

[79] Petrovskaya LE, Lukashev EP, Chupin VV, Sychev SV, Lyukmanova EN, Kryukova EA, Ziganshin RH, Spirina EV, Rivkina EM, Khatypov RA, Erokhina LG, Gilichinsky DA, Shuvalov VA, Kirpichnikov MP. Predicted bacteriorhodopsin from *Exiguobacterium sibiricum* is a functional proton pump. FEBS Letters. 2010;**584**: 4193-4196. DOI: 10.1016/j.febslet.2010.09.005

[80] Balashov SP, Imasheva ES, Boichenko VA, Antón J, Wang JM, Lanyi JK. Xanthorhodopsin: a proton pump with a light-harvesting carotenoid antenna. Science. 2005;**309**:2061-2064. DOI: 10.1126/science.1118046

[81] Lanyi JK, Balashov SP. Xanthorhodopsin: a bacteriorhodopsin-like proton pump with a carotenoid antenna. Biochimica et Biophysica Acta. 2008;**1777**:684-688. DOI: 10.1016/j.bbabio.2008.05.005

[82] Imasheva ES, Balashov SP, Choi AR, Jung KH, Lanyi JK. Reconstitution of *Gloeobacter violaceus* rhodopsin with a light-harvesting carotenoid antenna. Biochemistry. 2009;**48**:10948-10955. DOI: 10.1021/bi901552x

[83] Miranda MRM, Choi AR, Shi L, Bezerra Jr. AG, Jung KH, Brown LS. The photocycle and proton translocation pathway in a cyanobacterial ion-pumping rhodopsin. Biophysical Journal. 2009;**96**:1471-1481. DOI: 10.1016/j.bpj.2008.11.026

[84] Frigaard NU, Martinez A, Mincer TJ, DeLong EF. Proteorhodopsin lateral gene transfer between marine planktonic Bacteria and Archaea. Nature. 2006;**439**:847-850. DOI: 10.1038/nature04435

[85] Iverson V, Morris RM, Frazar CD, Berthiaume CT, Morales RL, Armbrust EV. Untangling genomes from metagenomes: revealing an uncultured class of marine euryarchaeota. Science. 2012;**335**: 587-590. DOI: 10.1126/science.1212665.

[86] Slamovits CH, Okamoto N, Burri L, James ER, Keeling PJ. A bacterial proteorhodopsin proton pump in marine eukaryotes. Nature Communications. 2011;**2**:183. DOI: 10.1038/ncomms1188

[87] Bieszke JA, Braun EL, Bean LE, Kang S, Natvig DO, Borkovich KA. The *nop-1* gene of *Neurospora crassa* encodes a seven transmembrane helix retinal-binding protein homologous to archaeal rhodopsins. Proceedings of the National Academy of Sciences of the United States of America. 1999;**96**:8034-8039. DOI: 10.1073/pnas.96.14.8034

[88] Bieszke JA, Spudich EN, Scott KL, Borkovich KA, Spudich JL. A eukaryotic protein, NOP-1, binds retinal to form an archaeal rhodopsin-like photochemically reactive pigment. Biochemistry. 1999;**38**:14138-14145. DOI: 10.1021/bi9916170

[89] Bieszke JA, Li L, Borkovich KA. The fungal opsin gene nop-1 is negatively-regulated by a component of the blue light sensing pathway and influences conidiation-specific gene expression in *Neurospora crassa*. Current Genetics. 2007;**52**:149-157. DOI: 10.1007/s00294-007-0148-8

[90] Estrada AF, Avalos J. Regulation and targeted mutation of opsA, coding for the NOP-1 opsin orthologue in *Fusarium fujikuroi*. Journal of Molecular Biology. 2009;**387**:59-73. DOI: 10.1016/j.jmb.2009.01.057

[91] Waschuk SA, Bezerra AG, Shi L, Brown LS. *Leptosphaeria* rhodopsin: bacteriorhodopsin-like proton pump from a eukaryote. Proceedings of the National Academy of Sciences of the United States of America. 2005;**102**: 6879-6883. DOI: 10.1073/pnas.0409659102

[92] Fan Y, Solomon P, Oliver RP, Brown LS. Photochemical characterization of a novel fungal rhodopsin from *Phaeosphaeria nodorum*. Biochimica et Biophysica Acta. 2011; **1807**:1457-1466. DOI: 10.1016/j.bbabio.2011.07.005

[93] Tsunoda SP, Ewers D, Gazzarrini S, Moroni A, Gradmann D, Hegemann P. H^+-pumping rhodopsin from the marine alga *Acetabularia*. Biophysical Journal.

2006;**91**:1471-1479. DOI: 10.1529/biophysj.106.086421

[94] Henry IM, Wilkinson MD, Hernandez JM, Schwarz-Sommer Z, Grotewold E. Mandoli DF. Comparison of ESTs from juvenile and adult phases of the giant unicellular green alga *Acetabularia acetabulum*. BMC Plant Biology. 2004;**4**:3. DOI: 10.1186/1471-2229-4-3

[95] Lee SS, Choi AR, Kim SY, Kang HW, Jung KH, Lee JH. *Acetabularia* rhodopsin I is a light-stimulated proton pump. Journal of Nanoscience and Nanotechnology. 2011; **11**:4596-4600. DOI:10.1166/jnn.2011.3650

[96] Wada T, Shimono K, Kikukawa T, Hato M, Shinya N, Kim SY, Kimura-Someya T, Shirouzu M, Tamogami J, Miyauchi S, Jung KH, Kamo N, Yokoyama S. Crystal structure of the eukaryotic light-driven proton-pumping rhodopsin, *Acetabularia* rhodopsin II, from marine alga. Journal of Molecular Biology. 2011;**411**: 986-998. DOI: 10.1016/j.jmb.2011.06.028

[97] Mogi T, Stern LJ, Marti T, Chao BH, Khorana HG. Aspartic acid substitutions affect proton translocation by bacteriorhodopsin. Proceedings of the National Academy of Sciences of the United States of America. 1988;**85**: 4148-4152. DOI: 10.1073/pnas.85.12.4148

[98] Garczarek F, Brown LS, Lanyi JK, Gerwert K. Proton binding within a membrane protein by a protonated water cluster. Proceedings of the National Academy of Sciences of the United States of America. 2005;**102**: 3633-3638. DOI: 10.1073/pnas.0500421102

[99] Garczarek F, Gerwert K. Functional waters in intraprotein proton transfer monitored by FTIR difference spectroscopy. Nature. 2006;**439**: 109-112. DOI: 10.1038/nature04231

[100] Zimányi L, Váró G, Chang M, Ni B, Needleman R, Lanyi JK. Pathways of proton release in the bacteriorhodopsin photocycle. Biochemistry. 1992;**31**:8535-8543. DOI: 10.1021/bi00151a022

[101] Balashov SP, Lu M, Imasheva ES, Govindjee R, Ebrey TG, Othersen III B, Chen Y, Crouch RK, Menick DR. The proton release group of bacteriorhodopsin controls the rate of the final step of its photocycle at low pH. Biochemistry. 1999;**38**:2026-2039. DOI: 10.1021/bi981926a

[102] Russell TS, Coleman M, Rath P, Nilsson A, Rothschild KJ. Threonine-89 participates in the active site of bacteriorhodopsin: evidence for a role in color regulation and Schiff base proton transfer. Biochemistry. 1997;**36**: 7490-7497. DOI: 10.1021/bi970287l

[103] Kandori H, Yamazaki Y, Shichida Y, Raap J, Lugtenburg J, Belenky M, Herzfeld J. Tight Asp-85–Thr-89 association during the pump switch of bacteriorhodopsin. Proceedings of the National Academy of Sciences of the United States of America. 2001;**98**:1571-1576. DOI: 10.1073/pnas.98.4.1571

[104] Luecke H. Atomic resolution structures of bacteriorhodopsin photocycle intermediates: the role of discrete water molecules in the function of this light-driven ion pump. Biochimica et Biophysica Acta. 2000; **1460**:133-156. DOI: 10.1016/S0005-2728(00)00135-3

[105] Dioumaev AK, Brown LS, Shih J, Spudich EN, Spudich JL, Lanyi JK. Proton transfers in the photochemical reaction cycle of proteorhodopsin. Biochemistry. 2002;**41**:5348-5358. DOI: 10.1021/bi025563x

[106] Friedrich T, Geibel S, Kalmbach R, Chizhov I, Ataka K, Heberle J, Engelhard M, Bamberg E. Proteorhodopsin is a light-driven proton pump with variable vectoriality. Journal of Molecular Biology. 2002;**321**:821-838. DOI: 10.1016/S0022283602006964

[107] Krebs RA, Dunmire D, Partha R, Braiman MS. Resonance Raman characterization of proteorhodopsin's chromophore environment. The Journal of Physical Chemistry B. 2003;107: 7877-7883. DOI: 10.1021/jp034574c

[108] Váró G, Brown LS, Lakatos M, Lanyi JK. Characterization of the photochemical reaction cycle of proteorhodopsin. Biophysical Journal. 2003;**84**:1202-1207. DOI: 10.1016/ S0006-3495(03)74934-0

[109] Lakatos M, Lanyi JK, Szakács J, Váró G. The photochemical reaction cycle of proteorhodopsin at low pH. Biophysical Journal. 2003;**84**:3252-3256. DOI: 10.1016/S0006-3495(03)70049-6

[110] Bergo V, Amsden JJ, Spudich EN, Spudich JL, Rothschild KJ. Structural changes in the photoactive site of proteorhodopsin during the primary photoreaction. Biochemistry. 2004;**43**: 9075-9083. DOI: 10.1021/bi0361968

[111] Ludmann K, Gergely C, Váró G. Kinetic and thermodynamic study of the bacteriorhodopsin photocycle over a wide pH range. Biophysical Journal. 1998;**75**: 3110-3119. DOI: 10.1016/ S0006-3495(98)77752-5

[112] Fujisawa T, Abe M, Tamogami J, Kikukawa T, Kamo N, Unno M. Low-temperature Raman spectroscopy reveals small chromophore distortion in primary photointermediate of proteorhodopsin. FEBS Letters. 2018; **592**:3054-3061. DOI: 10.1002/ 1873-3468.13219

[113] Wang WW, Sineshchekov OA, Spudich EN, Spudich JL. Spectroscopic and photochemical characterization of a deep ocean proteorhodopsin. The Journal of Biological Chemistry. 2003; **278**:33985-33991. DOI: 10.1074/jbc. M305716200

[114] Balashov SP, Petrovskaya LE, Imasheva ES, Lukashev EP, Dioumaev AK, Wang JM, Sychev SV, Dolgikh DA, Rubin AB, Kirpichnikov MP, Lanyi JK. Breaking the carboxyl rule: Lysine 96 facilitates reprotonation of the Schiff base in the photocycle of a retinal protein from *Exiguobacterium sibiricum*. The Journal of Biological Chemistry. 2013;**288**: 21254-21265 DOI: 10.1074/jbc. M113.465138

[115] Petrovskaya LE, Balashov SP, Lukashev EP, Imasheva ES, Gushchin IY, Dioumaev AK, Rubin AB, Dolgikh DA, Gordeliy VI, Lanyi JK, Kirpichnikov MP. ESR - a retinal protein with unusual properties from *Exiguobacterium sibiricum*. Biochemistry (Moscow). 2015;**80**:688-700. DOI: 10.1134/S000629791506005X

[116] Nakamura S, Kikukawa T, Tamogami J, Kamiya M, Aizawa T, Hahn MW, Ihara K, Kamo N, Demura M. Photochemical characterization of actinorhodopsin and its functional existence in the natural host. Biochimica et Biophysica Acta. 2016;**1857**:1900-1908. DOI: 10.1016/j. bbabio.2016.09.006

[117] Klyszejko AL, Shastri S, Mari SA, Grubmüller H, Muller DJ, Glaubitz C. Folding and assembly of proteorhodopsin. Journal of Molecular Biology. 2008;**376**:35-41. DOI: 10.1016/j. jmb.2007.11.030

[118] Luecke H, Schobert B, Stagno J, Imasheva ES, Wang JM, Balashov SP, Lanyi JK. Crystallographic structure of xanthorhodopsin, the light-driven proton pump with a dual chromophore. Proceedings of the National Academy of Sciences of the United States of

America. 2008;**105**:16561-16565. DOI: 10.1073_pnas.0807162105

[119] Pfleger N, Wörner AC, Yang J, Shastri S, Hellmich UA, Aslimovska L, Maier MSM, Glaubitz C. Solid-state NMR and functional studies on proteorhodopsin. Biochimica et Biophysica Acta. 2009;**1787**:697-705. DOI: 10.1016/j.bbabio.2009.02.022

[120] Reckel S, Gottstein D, Stehle J, Lchr F, Verhoefen MK, Takeda M, Silvers R, Kainosho M, Glaubitz C, Wachtveitl J, Bernhard F, Schwalbe H, Güntert P, Dötsch V. Solution NMR structure of proteorhodopsin. Angewandte Chemie International Edition. 2011;**50**:1-6. DOI: 10.1002/anie.201105648

[121] Ran T, Ozorowski G, Gao Y, Sineshchekov OA, Wang W, Spudich JL, Luecke H. Cross-protomer interaction with the photoactive site in oligomeric proteorhodopsin complexes. Acta Crystallographica Section D: Structural Biology. 2013;**D69**: 1965-1980. DOI: 10.1107/S0907444913017575

[122] Gushchin I, Chervakov P, Kuzmichev P, Popov AN, Round E, Borshchevskiy V, Ishchenko A, Petrovskaya L, Chupin V, Dolgikh DA, Arseniev AS, Kirpichnikov M, Gordeliy V. Structural insights into the proton pumping by unusual proteorhodopsin from nonmarine bacteria. Proceedings of the National Academy of Sciences of the United States of America. 2013;**110**: 12631-12636. DOI: 10.1073/pnas.1221629110

[123] Morizumi T, Ou WL, Eps NV, Inoue K, Kandori H, Brown LS, Ernst OP. X-ray crystallographic structure and oligomerization of *Gloeobacter* rhodopsin. Scientific Reports. 2019;**9**:11283. DOI: 10.1038/s41598-019-47445-5

[124] Brown LS. Fungal rhodopsins and opsin-related proteins: eukaryotic homologues of bacteriorhodopsin with unknown functions. Photochemical & Photobiological Sciences. 2004;**3**: 555-565. DOI: 10.1039/ b315527g

[125] Sumii M, Furutani Y, Waschuk SA, Brown LS, Kandori H. Strongly hydrogen-bonded water molecule present near the retinal chromophore of *Leptosphaeria* rhodopsin, the bacteriorhodopsin-like proton pump from a eukaryote. Biochemistry. 2005; **44**:15159-15166. DOI: 10.1021/bi0513498

[126] Furutani Y, Sumii M, Fan Y, Shi L, Waschuk SA, Brown LS, Kandori H. Conformational coupling between the cytoplasmic carboxylic acid and the retinal in a fungal light-driven proton pump. Biochemistry. 2006;**45**: 15349-15358. DOI: 10.1021/bi061864l

[127] Fan Y, Shi L, Brown LS. Structural basis of diversification of fungal retinal proteins probed by site-directed mutagenesis of *Leptosphaeria* rhodopsin. FEBS Letters. 2007;**581**:2557-2561. DOI: 10.1016/j.febslet.2007.05.001

[128] Ito H, Sumii M, Kawanabe A, Fan Y, Furutani Y, Brown LS, Kandori H. Comparative FTIR study of a new fungal rhodopsin. The Journal of Physical Chemistry B. 2012;**116**: 11881-11889. DOI: 10.1021/jp306993a

[129] Shimono K, Goto M, Kikukawa T, Miyauchi S, Shirouzu M, Kamo N, Yokoyama S. Production of functional bacteriorhodopsin by an *Escherichia coli* cell-free protein synthesis system supplemented with steroid detergent and lipid. Protein Science. 2009;**18**: 2160-2171. DOI: 10.1002/pro.230

[130] Kikukawa T, Shimono K, Tamogami J, Miyauchi S, Kim SY, Kimura-Someya T, Shirouzu M, Jung KH, Yokoyama S, Kamo N. Photochemistry of *Acetabularia*

rhodopsin II from a marine plant, *Acetabularia acetabulum*. Biochemistry. 2011;**50**:8888-8898. DOI: 10.1021/bi2009932

[131] Furuse M, Tamogami J, Hosaka T, Kikukawa T, Shinya N, Hato M, Ohsawa N, Kim SY, Jung KH, Demura M, Miyauchi S, Kamo N, Shimono K, Kimura-Someya T, Yokoyama S, Shirouzu M. Structural basis for the slow photocycle and late proton release in *Acetabularia* rhodopsin I from the marine plant *Acetabularia acetabulum*. Acta Crystallographica Section D: Structural Biology. 2015;D**71**: 2203-2216. DOI: 10.1107/S1399004715015722

[132] Tamogami J, Kikukawa T, Nara1 T, Demura M, Kimura-Someya T, Shirouzu M, Yokoyama S, Miyauchi S, Shimono K, Kamo N. Existence of two O-like intermediates in the photocycle of *Acetabularia* rhodopsin II, a light-driven proton pump from a marine alga. Biophysics and Physicobiology. 2017;**14**: 49-55. DOI: 10.2142/biophysico.14.0_49

[133] Tamogami J, Kikukawa T, Ohkawa K, Ohsawa N, Nara T, Demura M, Miyauchi S, Kimura-Someya T, Shirouzu M, Yokoyama S, Shimono K, Kamo N. Interhelical interactions between D92 and C218 in the cytoplasmic domain regulate proton uptake upon N-decay in the proton transport of *Acetabularia* rhodopsin II. Journal of Photochemistry & Photobiology, B: Biology. 2018;**183**: 35-45. DOI: 10.1016/j.jphotobiol.2018.04.012

[134] Balashov SP, lmasheva ES, Govindjee R, Ebrey TG. Titration of aspartate-85 in bacteriorhodopsin: What it says about chromophore isomerization and proton release. Biophysical Journal. 1996;**70**:473-481. DOI: 10.1016/S0006-3495(96)79591-7

[135] Imasheva ES, Balashov SP, Jennifer M. Wang JM, Lanyi JK. pH-dependent transitions in xanthorhodopsin. Photochemistry and Photobiology. 2006;**82**:1406-1413. DOI: 10.1562/2006-01-15-RA-776

[136] Tsukamoto T, Kikukawa T, Kurata T, Jung KH, Kamo N, Demura M. Salt bridge in the conserved His–Asp cluster in *Gloeobacter* rhodopsin contributes to trimer formation. FEBS Letters. 2013;**587**:322-327. DOI: 10.1016/j.febslet.2012.12.022

[137] Balashov SP, Petrovskaya LE, Lukashev EP, Imasheva ES, Dioumaev AK, Wang JM, Sychev SV, Dolgikh DA, Rubin AB, Kirpichnikov MP, Lanyi JK. Aspartate-histidine interaction in the retinal Schiff base counterion of the light-driven proton pump of *Exiguobacterium sibiricum*. Biochemistry. 2012;**51**: 5748-5762. DOI: 10.1021/bi300409m Biochemistry

[138] Partha R, Krebs R, Caterino TL, Braiman MS. Weakened coupling of conserved arginine to the proteorhodopsin chromophore and its counterion implies structural differences from bacteriorhodopsin. Biochimica et Biophysica Acta. 2005;**1708**:6-12. DOI: 10.1016/j.bbabio.2004.12.009

[139] Hempelmann F, Hölper S, Verhoefen MK, Woerner AC, Köhler T, Fiedler SA, Pfleger N, Wachtveitl J, Glaubitz C. His75-Asp97 cluster in green proteorhodopsin. Journal of the American Chemical Society. 2011;**133**: 4645-4654. DOI: 10.1021/ja111116a

[140] Lazarova T, Sanz C, Querol E, Padrós E. Fourier transform infrared evidence for early deprotonation of Asp85 at alkaline pH in the photocycle of bacteriorhodopsin mutants containing E194Q. Biophysical Journal. 2000;**78**:2022-2030. DOI: 10.1016/S0006-3495(00)76749-X

[141] Imasheva ES, Balashov SP, Wang JM, Dioumaev AK, Lanyi JK.

Selectivity of retinal photoisomerization in proteorhodopsin is controlled by aspartic acid 227. Biochemistry. 2004; 43:1648-1655. DOI: 10.1021/bi0355894

[142] Xiao Y, Partha R, Krebs R, Braiman M. Time-resolved FTIR spectroscopy of the photointermediates involved in fast transient H^+ release by proteorhodopsin. The Journal of Physical Chemistry B. 2005;**109**: 634-641. DOI: 10.1021/jp046314g

[143] Bergo VB, Sineshchekov OA, Kralj JM, Partha R, Spudich EN, Rothschild KJ, Spudich JL. His-75 in proteorhodopsin, a novel component in light-driven proton translocation by primary pumps. The Journal of Biological Chemistry. 2009;**284**:2836–2843. DOI: 10.1074/jbc.M803792200

[144] Ikeda D, Furutani Y, Kandori H. FTIR study of the retinal Schiff base and internal water molecules of proteorhodopsin. Biochemistry. 2007; **46**:5365-5373. DOI: 10.1021/bi700143g

[145] Tamogami T, Kikukawa T, Nara T, Shimono K, Demura M, Kamo N. Photoinduced proton release in proteorhodopsin at low pH: the possibility of a decrease in the pK_a of Asp227. Biochemistry. 2012;**51**: 9290-9301. DOI: 10.1021/bi300940p

[146] Bondar AN, Elstner M, Suhai S, Smith JC, Fischer S. Mechanism of primary proton transfer in bacteriorhodopsin. Structure. 2004;**12**: 1281-1288. DOI: 10.1016/j.str.2004.04.016

[147] Brown LS, Lanyi JK. Determination of the transiently lowered pK_a of the retinal Schiff base during the photocycle of bacteriorhodopsin. Proceedings of the National Academy of Sciences of the United States of America. 1996;**93**: 1731-1734. DOI: 10.1073/pnas.93.4.1731

[148] Szaraz S, Oesterhelt D, Ormos P. pH-induced structural changes in bacteriorhodopsin studied by Fourier transform infrared spectroscopy. Biophysical Journal. 1994;**67**: 1706-1712. DOI: 10.1016/S0006-3495(94)80644-7

[149] Zscherp C, Schlesinger R, Tittor J, Oesterhelt D, Heberle J. In situ determination of transient pK_a changes of internal amino acids of bacteriorhodopsin by using timeresolved attenuated total reflection Fourier-transform infrared spectroscopy. Proceedings of the National Academy of Sciences of the United States of America. 1999;**96**: 5498-5503. DOI: 10.1073/pnas.96.10.5498

[150] Dioumaev AK, Brown LS, Needleman R, Lanyi JK. Coupling of the reisomerization of the retinal, proton uptake, and reprotonation of Asp-96 in the N photointermediate of bacteriorhodopsin. Biochemistry. 2001; **40**:11308-11317. DOI: 10.1021/bi011027d

[151] Luecke H, Schobert B, Cartailler JP, Richter HT, Rosengarth A, Needleman R, Lanyi JK. Coupling photoisomerization of retinal to directional transport in bacteriorhodopsin. Journal of Molecular Biology. 2000;**300**:1237-1255. DOI: 10.1006/jmbi.2000.3884

[152] Harris A, Ljumovic M, Bondar AN, Shibata Y, Ito S, Inoue K, Kandori H, Brown LS. A new group of eubacterial light-driven retinal-binding proton pumps with an unusual cytoplasmic proton donor. Biochimica et Biophysica Acta. 2015;**1847**:1518-1529. DOI: 10.1016/j.bbabio.2015.08.003

[153] Sudo Y, Yoshizawa S. Functional and photochemical characterization of a light-driven proton pump from the Gammaproteobacterium *Pantoea vagans*. Photochemistry and Photobiology. 2016;**92**:420-427. DOI: 10.1111/php.12585

[154] Dyukova T, Robertson B, Weetall H. Optical and electrical characterization of bacteriorhodopsin films. Biosystems. 1997;**41**:91-98. DOI: 10.1016/S0303-2647(96)01665-6

[155] Wang T, Sessions AO, Lunde CS, Rouhani S, Glaeser RM, Duan Y, Facciotti MT. Deprotonation of D96 in bacteriorhodopsin opens the proton uptake pathway. Structure. 2013;**21**: 290-297. DOI: 10.1016/j.str.2012.12.018

[156] Haupts U, Tittor J, Bamberg E, Oesterhelt D. General concept for ion translocation by halobacterial retinal proteins: the isomerization/switch/ transfer (IST) model. Biochemistry. 1997;**36**:2-7. DOI: 10.1021/bi962014g

[157] Wang T, Facciotti MT, Duan Y. Schiff base switch II precedes the retinal thermal isomerization in the photocycle of bacteriorhodopsin. PLoS One. 2013;**8**: e69882. DOI: 10.1371/journal. pone.0069882

[158] Delaney JK, Schweiger U, Subramaniam S. Molecular mechanism of protein-retinal coupling in bacteriorhodopsin. Proceedings of the National Academy of Sciences of the United States of America. 1995;**92**: 11120-11124. DOI: 10.1073/ pnas.92.24.11120

[159] Iwamoto M, Sudo Y, Shimono K, Araiso T, Kamo N. Correlation of the O-Intermediate rate with the pK_a of Asp-75 in the dark, the counterion of the Schiff base of pharaonis phoborhodopsin (sensory rhodopsin II). Biophysical Journal. 2005;**88**:1215-1223. DOI: 10.1529/biophysj.104.045583

[160] Miyasaka T, Koyama K, Itoh I. Quantum conversion and image detection by a bacteriorhodopsin-based artificial photoreceptor. Science. 1992; **255**:342-344. DOI: 10.1126/ science.255.5042.342

[161] Robertson B, Lukashev EP. Rapid pH change due to bacteriorhodopsin measured with a tin-oxide electrode. Biophysical Journal. 1995;**68**:1507-1517. DOI: 10.1016/S0006-3495(95)80323-1

[162] Tamogami J, Kikukawa T, Miyauchi S, Muneyuki E, Kamo N. A tin oxide transparent electrode provides the means for rapid time-resolved pH measurements: application to photoinduced proton transfer of bacteriorhodopsin and proteorhodopsin. Photochemistry and Photobiology. 2009;**85**:578-589. DOI: 10.1111 / j.1751-1097.2008.00520.x

[163] Wu J, Ma D, Wang Y, Ming M, Balashov SP, Ding J. Efficient approach to determine the pK_a of the proton release complex in the photocycle of retinal proteins. The Journal of Physical Chemistry B. 2009;**113**:4482-4491. DOI: 10.1021/jp804838h

[164] Tamogami J, Sato K, Kurokawa S, Yamada T, Nara T, Demura M, Miyauchi S, Kikukawa T, Muneyuki E, Kamo N. Formation of M-like intermediates in proteorhodopsin in alkali solutions (pH $\geq \sim$8.5) where the proton release occurs first in contrast to the sequence at lower pH. Biochemistry. 2016;**55**:1036-1048. DOI: 10.1021/acs. biochem.5b01196

[165] Tsukamoto T, Inoue K, Kandori H, Sudo Y. Thermal and spectroscopic characterization of a proton pumping rhodopsin from an extreme thermophile. The Journal of Biological Chemistry. 2013;**288**:21581-21592. DOI: 10.1074/jbc.M113.479394

[166] Kanehara K, Yoshizawa S, Tsukamoto T, Sudo Y. A phylogenetically distinctive and extremely heat stable light-driven proton pump from the eubacterium *Rubrobacter xylanophilus* DSM 9941^T. Scientific Reports. 2017;**7**:44427. DOI: 10.1038/srep44427

[167] Beppu K, Sasaki T, Tanaka KF, Yamanaka A, Fukazawa Y,

Shigemoto R, Matsui K. Optogenetic countering of glial acidosis suppresses glial glutamate release and ischemic brain damage. Neuron. 2014;**81**:314-320. DOI: 10.1016/j.neuron.2013.11.011

[168] Rost BR, Schneider F, Grauel MK, Wozny C, Bentz CG, Blessing A, Rosenmund T, Jentsch TJ, Schmitz D, Hegemann P, Rosenmund C. Optogenetic acidification of synaptic vesicles and lysosomes. Nature Neuroscience. 2015;**18**:1845-1852. DOI: 10.1038/nn.4161

[169] Hara KY, Wada T, Kino K, Asahi T, Sawamura N. Construction of photoenergetic mitochondria in cultured mammalian cells. Scientific Reports. 2013;**3**:1635. DOI: 10.1038/srep01635

[170] Brown J, Behnam R, Coddington L, Tervo DGR, Martin K, Proskurin M, Kuleshova E, Park J, Phillips J, Bergs ACF, Gottschalk A, Dudman JT, Karpova AY. Expanding the optogenetics toolkit by topological inversion of rhodopsins. Cell. 2018;**175**: 1-10. DOI: 10.1016/j.cell.2018.09.026

[171] Inoue K, Ito S, Kato Y, Nomura Y, Shibata M, Uchihashi T, Tsunoda SP, Kandori H. A natural light-driven inward proton pump. Nature Communications. 2016;**7**:13415. DOI: 10.1038/ncomms13415

[172] Inoue K, Tsunoda SP, Singh M, Tomida S, Hososhima S, Konno M, Nakamura R, Watanabe H, Bulzu PA, Banciu HL, Andrei AS, Uchihashi T, Ghai R, Béjà O, Kandori H. Schizorhodopsins: a family of rhodopsins from Asgard archaea that function as light-driven inward H^+ pumps. Science Advances. 2020;**6**: eaaz2441. DOI: 10.1126/sciadv.aaz2441

[173] Altan N, Chen Y, Schindler M, Simon SM. Defective acidification in human breast tumor cells and implications for chemotherapy. Journal of Experimental Medicine. 1998;**187**: 1583-1598. DOI: 10.1084/jem.187.10.1583

[174] Gong Y, Duvvuri M, Krise JP. Separate roles for the Golgi apparatus and lysosomes in the sequestration of drugs in the multidrug-resistant human leukemic cell line HL-60. The Journal of Biological Chemistry. 2003;**278**: 50234-50239. DOI: 10.1074/jbc.M306606200